

The Propulsion Committee

Final Report and Recommendations to the 25th ITTC

1. INTRODUCTION

1.1 Membership and Meetings

The members of the Propulsion Committee of the 25th International Towing Tank Conference are as follows:

- Dr. Ki-Han Kim (Chairman), Office of Naval Research (ONR), U.S.A.
- Dr. Stephen Turnock (Secretary), University of Southampton, U.K.
- Professor Jun Ando, Kyushu University, Japan
- Dr. Paolo Becchi, CETENA, Italy
- Professor Emin Korkut, Technical University of Istanbul, Turkey
- Dr. Anton Minchev, FORCE Technology, Denmark
- Ms. Elena Ya Semionicheva, Krylov Shipbuilding Research Institute, Russia
- Dr. Suak-Ho Van, Maritime and Ocean Engineering Research Institute (MOERI), Korea
- Dr. Wei-Xin Zhou, China Ship Scientific Research Center (CSSRC), China.

Four Committee meetings were held as follows:

- Technical University of Istanbul, Turkey, 1-3 February 2006
- CETENA, Italy, 25-27 September 2006
- David Taylor Model Basin, USA, 18-20 April 2007
- FORCE Technology, Denmark, 23-25 October 2007.

1.2 Recommendations of the 24th ITTC

The 24th ITTC recommended the following work for the 25th ITTC Propulsion Committee:

1. Update the state-of-the-art for propulsion systems emphasizing developments since the 2005 ITTC conference.
 - (a) Comment on the potential impact of new developments on the ITTC,
 - (b) Emphasize new experimental techniques and extrapolation methods and the practical application of computational methods to performance prediction and scaling,
 - (c) Identify the need for R&D for improving methods of model experiments, numerical modelling and full-scale measurements.
2. Review the following ITTC recommended procedures:
 - 7.5-01-02-01: Terminology and Nomenclature of Propeller Geometry (Harmonize with ISO standard)
 - 7.5-02-03-01.1: Propulsion Test
 - 7.5-02-03-02.1: Propeller Open Water Test
 - 7.5-02-03-02.3: Guide for Use of LDV
 - 7.5-02-05-02: High Speed Marine Vehicles Propulsion Test.
 - (a) Determine if any changes are needed in the light of current practice.



- (b) In the review and update of the existing propeller open water test procedure 7.5-02-03-02.1 its applicability to new types of propulsors should be taken into account.
 - (c) Identify the requirements for new procedures.
 - (d) Support the Specialist Committee on Uncertainty Analysis in reviewing the procedures handling uncertainty analysis.
3. Critically review examples of validation of prediction techniques. Identify and specify requirements for new benchmark data.
 4. Review the development and progress in unconventional propulsors such as tip-rake, transcavitating and composite propellers (hydroelasticity and cavitation erosion susceptibility taken into account).
 5. Review propulsion issues in shallow water and formulate recommendations for research.
 6. Review the methods for predicting the performance of secondary thrusters and compare with operational experience.
 7. Finalise the benchmark tests for waterjets and analysis of the data.

1.3 General Remarks

The Propulsion Committee addressed all the tasks assigned to it with different degrees of completeness. The initial review of the above recommendations revealed that there is an overlapping aspect in Recommendations 1.(a) and 1.(b) above. The Committee recommended to the Advisory Council that the original 1.(a) be dropped and 1.(b) be modified to read, “Emphasize new propulsion concepts and experimental techniques and extrapolation methods and the practical application of computational methods to performance prediction

and scaling.” Both changes were approved by the Advisory Council.

The Propulsion Committee reviewed five procedures recommended by the ITTC. For the Guide for Use of LDV (7.5-02-03-02.3), the Committee decided that the current members do not possess expertise to provide proper guidance for use of LDV, thus limiting the scope of review for this task to reviewing papers on the applications of LDV and PIV. In view of increasing use of LDV and PIV in the cavitation tunnel and in the towing tank, the Committee recommends that a Specialist Committee on LDV/PIV be established to provide proper guidance for experimentalists. The review of the High Speed Marine Vehicles Propulsion Test (7.5-02-05-02) was challenging because of insufficient information in the existing document as well as in the literature. In this case mostly clarifications were made with no significant changes to the actual procedure. However, it should be recognised that a number of aspects of this procedure would benefit from more detailed research especially on the effect of shaft inclination on actual effective wake analysis.

There was a limited amount of recent material available in the public domain for work related to shallow water effects and in the performance of secondary thrusters. This has also limited the work of the Committee.

Although there have been a reasonable number of conferences during which a range of valuable contribution to the development of marine propulsion has been reported, there would appear to be a trend towards presentation of work based solely on computational fluid dynamic analysis without suitable experimental corroboration or occasionally without even attempts to examine the numerical sensitivity of the results. This is due in part to the difficulty of obtaining high quality experimental data and the large computational resources required but due care is required especially if the information is presented by organisations with a commercial interest.

2. UPDATE THE STATE-OF-THE-ART FOR PROPULSION SYSTEMS EMPHASISING DEVELOPMENTS SINCE THE 2005 ITTC CONFERENCE

2.1 Introduction

Several major international conferences were held since the 24th ITTC conference in 2005; CAV2006 (Sep. 2006, the Netherlands), Propellers/Shafting '06 (Sep. 2006, U.S.A.), 26th Symposium on Naval Hydrodynamics (Sep. 2006, Italy), T-POD 2006 (Oct. 2006, France), 9th International Conference on Numerical Ship Hydrodynamics (Aug. 2007, U.S.A.), FAST 2007 (Sep. 2007, China). Most relevant papers from these conferences and from other technical journals and conferences were reviewed and reported.

Advances in computational analysis of fluid flow, application of new materials to propulsion devices and developments in instrumentation were reported and have a direct effect on the way on which ITTC members conduct their propulsion related activities. Advances in computational tools and computer hardware enabled researchers to be able to compute the steady ship propulsion characteristics for fully appended ship hull with propeller operating and highly separated unsteady flow around propellers that have only been feasible through experiments until recently. These advances would contribute to the development of more efficient propellers with less cavitation and efficient hull forms with improved powering performance.

Although there were few new propulsion concepts or systems reported since the 24th ITTC Conference in 2005, continued improvements in the design, analysis and experimental methods were reported for tip-rake propellers, surface-piercing propellers, supercavitating propellers, and composite propellers. The progress in these unconventional propulsors is reviewed in Section 5.

Some new developments were reported in waterjets, podded propulsors and advanced blade section concepts. These new developments are reported in this Section.

2.2 Overview of New Developments

2.2.1 Axial-Flow Waterjet Significant advancements in waterjet technology have been reported in two areas; capability of computational tools for design and analysis and compact waterjet technology.

Kerwin (2006) presented a review of the current state-of-the-art experimental and computational hydrodynamics as applied to the design and analysis of waterjet propulsion systems. He concluded that a range of computational tools is beneficial - from fast and simple to computationally intensive. Progress in research might well benefit from greater interaction between the developers of different computational approaches.

Kerwin, *et al.* (2006) presented a unified approach to hydrodynamic design/analysis problem for a wide class of propulsors including ducted, podded and waterjets. The approach consists of a coupled axisymmetric flow/lifting surface representation of the total flow field. Once the approach is verified and validated, it can be used for a fast parametric study of waterjets, ducted propellers, and podded propellers with multiple blade rows.

New results were reported in the development of compact, axial-flow waterjet technology for high-speed commercial and naval ship applications. The current waterjet market is dominated by the mixed-flow waterjets. So why consider axial-flow waterjets? High-speed ships generally use slender hullforms to reduce the wave drag and require efficient, but compact, propulsion systems. Figure 2.1 illustrates the size comparison between the mixed-flow and axial-flow waterjets (Lavis, *et al.*, 2007). For the same inlet diameter and thus the same unit thrust, the axial-flow pump has a signifi-

cantly smaller transom footprint than the mixed flow pump. Therefore, for a given transom area, one can install more number of axial-flow waterjets or conversely, for the same total thrust, the use of axial-flow pumps can allow for a significantly reduced transom size and thus a significant reduction in wave drag for a high-speed ship.

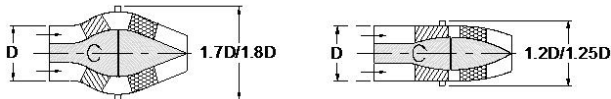


Figure 2.1 Comparison of mixed-flow (left) and axial-flow (right) waterjet dimensions (Lavis, *et al.*, 2007).

Lavis, *et al.* (2007) designed an axial-flow waterjet pump for a notional high-speed sealift ship that would be propelled by four 90-inch diameter axial-flow waterjets, each absorbing 57,330 hp. An extensive model-scale evaluation was performed at DTMB facility. A 7.5-inch model pump (1/12th scale) was tested in the cavitation tunnel (see Figure 2.2) and a self-propulsion test was conducted in the towing tank using a demi-hull of a representative large catamaran using two surrogate model pumps.



Figure 2.2 Pump performance testing at 24-inch water tunnel at DTMB using 7.5-inch diameter axial-flow pump (Lavis, *et al.*, 2007).

Brewton, *et al.* (2006) presented computations of steady performance (thrust, torque and efficiency) and detailed flow in the axial-flow pump designed by Lavis, *et al.* (2007) using RANS code with a mixing-plane approach.

Figure 2.3 shows the computer image of the axial-flow waterjet. Figure 2.4 shows a comparison between the computations and measurements of headrise and efficiency as a function of flow rate. The agreement between RANS computations and measurements is very good.

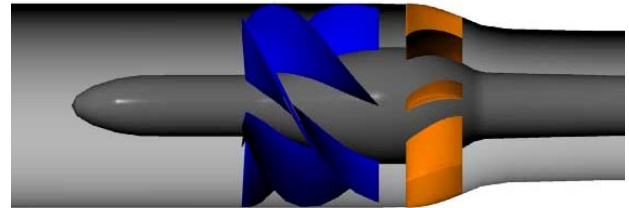


Figure 2.3 Axial-flow waterjet pump for RANS flow computations (Brewton, *et al.*, 2006).

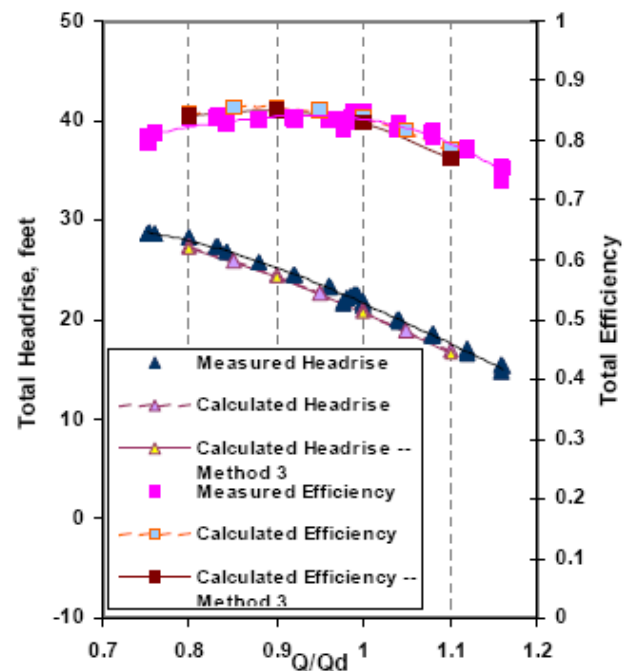


Figure 2.4 Comparison of headrise and pump efficiency between RANS computations and measurements (Brewton, *et al.*, 2006).

Kinnas, *et al.* (2007) developed a potential-flow computational method to predict the performance of a cavitating waterjet by extending their boundary element method (BEM) for cavitating ducted propeller performance prediction (Lee and Kinnas, 2006). As part of their

validation efforts, they also computed the performance of the axial-flow pump designed by Lavis, *et al.* (2007). The computed torque values were significantly lower than the experiments. The authors attributed the discrepancy to the lack of proper modelling of the gap flow and to the simple viscous model in their BEM code. Further verification and validation is required to confirm this.

Bulten and Verbeek (2007) presented a development of an axial-flow waterjet at Wärtsilä company. The cavitation performance of the axial-flow pump in terms of cavitation margin was significantly better than the equivalent mixed-flow pump with similar efficiency. Based on the extensive computational and experimental efforts, Wärtsilä developed two commercial axial-flow pump series LJX and WLD and made them available in the market.

The U.S. Navy is engaged in the development of axial-flow pump technologies for applications to large high-speed naval ships. Fung, *et al.* (2007) developed a notional mono-hull design of a high-speed sealift ship with different bow and stern configurations to evaluate the powering performance of different propulsor configurations, including the axial-flow and mixed-flow waterjets, podded propulsors and the conventional open propellers with shafts and struts. Resistance tests showed that the hull form for the axial-flow waterjet was most favorable (Cusanelli, *et al.*, 2007). Powering tests confirmed that waterjets performed better for higher speed range than conventional open propellers and that for lower speed range the conventional open propellers performed better. Figure 2.5 shows the stern of the model hull with four axial-flow waterjets and inlets. Figure 2.6 shows the model powering test in the towing tank at 39 knots full-scale speed.

2.2.2 Podded Propulsors Following the first podded propulsor conference in 2004 (T-POD 2004), the second one (T-POD 2006) was held in 2006 in France where continued progresses in the design and analysis capabilities, open-water and propulsion test procedures,

powering performance predictions were presented.



Figure 2.5 Axial-flow waterjets and inlets for a notional high-speed sealift ship (Cusanelli, *et al.*, 2007).



Figure 2.6 Powering test of a high-speed sealift ship with four axial-flow waterjets (Cusanelli, *et al.*, 2007).

The contributions to the second T-POD conference can be grouped in four major technical areas: (1) Investigation of influence of various podded propulsor geometrical particulars on the performance, Islam, *et al.* (2006) and Frolova, *et al.* (2006); (2) Podded propulsor model testing procedure and full-scale powering prediction, Flikkema, *et al.* (2006); (3) Podded propulsor simulations using CFD, Greco, *et al.* (2006), Sánchez-Caja, *et al.* (2006b), Kinnas (2006) and Deniset, *et al.* (2006); and (4) Podded propulsor scale effect studies through numerical simulations, Krasilnikov, *et al.* (2006).



2.2.3 Advanced Blade Sections: Conventional propellers are inefficient at high speed primarily due to significant blade cavitation. Increasing demand for high speed ships motivates the development of efficient propulsors at both low and high speed. Several papers on advanced blade sections that would perform well in both low and high speed regimes have recently been presented. Figure 2.7 shows a general trend of efficiency as a function of ship speed for different types of propulsors (Black, *et al.*, 2006).

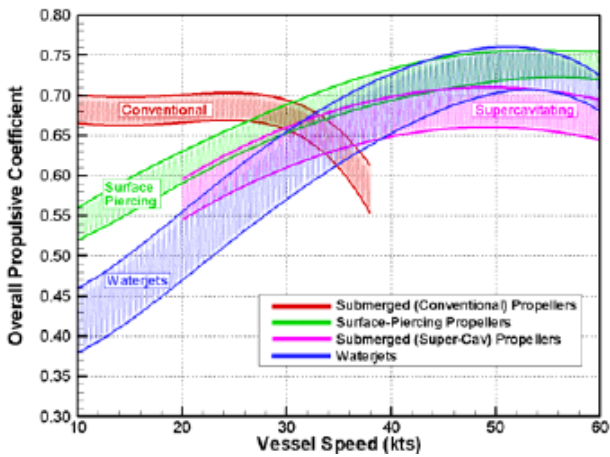


Figure 2.7 Overall propulsive coefficient versus ship speed for different propulsor types (Black, *et al.*, 2006).

Black, *et al.* (2006) developed new blade section concepts that have the efficiency characteristics of conventional submerged sub-cavitating propellers at low and intermediate speeds but can transition to a super-cavitating mode for high speed operation without encountering thrust breakdown (see Figure 2.8).

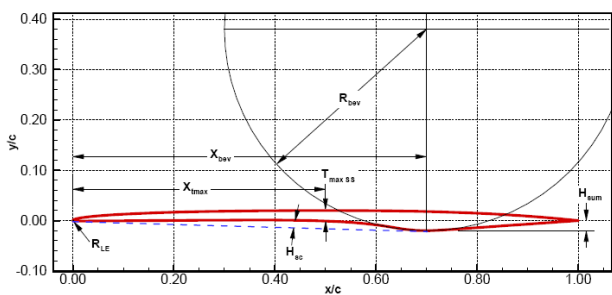


Figure 2.8 Geometric parameters for advanced blade section definition (Black, *et al.*, 2006).

Using the 2-D section shape in Figure 2.8, a notional new propeller design was developed for a Patrol Craft (see Figure 2.9). The new design retained the same skew, chord, rake and spanwise loading as the parent propeller. The computational results for the required horsepower for the new propeller compared to the non-cavitating parent propeller are shown in Figure 2.10. At 20 knots, both propellers were predicted to operate at the same efficiency and RPM. At 39 knots, the parent propeller requires 23% more horsepower than the new design.



Figure 2.9 Patrol Craft with 4 parent propellers (Black, *et al.*, 2006).

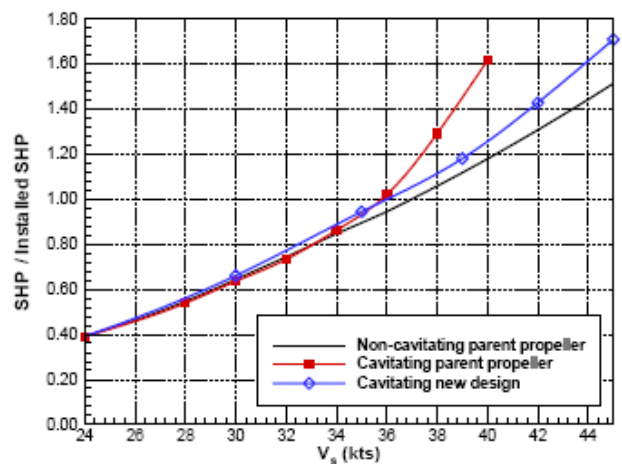


Figure 2.10 Required shaft horsepower versus speed for a Patrol Craft propeller (Black, *et al.*, 2006).

A similar concept called a dual-cavitating propeller was proposed by Young and Shen (2007). This propeller concept is based on the

dual-cavitating hydrofoil section developed by Shen (1996) that is capable of operating efficiently at low- and mid-speeds in subcavitating (fully wetted) mode, and at high-speeds in the supercavitating mode (see Figure 2.11). The authors developed a numerical tool based on BEM to predict the hydrodynamic and hydro-elastic response of propellers in subcavitating, partially cavitating, and supercavitating conditions. The authors applied the numerical tool to predict the performance of the well-known Newton-Rader (1961) propeller that has blade sections similar to the dual-cavitating blade sections. The predicted cavitation patterns, blade forces, stress distributions, blade deflections, and dynamic characteristics in various cavitating conditions were in good agreement with measurements.

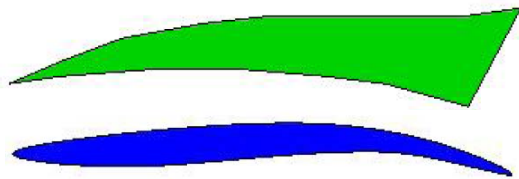


Figure 2.11 Comparison of SCP/SPP blade section (upper) and the dual-cavitating blade section (lower) (Young and Shen, 2007).

2.2.4 Full Scale Measurements

Despite the importance of the full scale data, published data are scarce due to the cost and difficulties associated with full scale tests.

The most notable full-scale measurements were performed recently as part of the EROCAV (EROsion on Ship Propellers and Rudders - the Influence of CAVitation on Material Damages) project. Full scale cavitation observation and erosion data for five ships were obtained in this project. An executive summary of the EROCAV Project can be found in the 24th ITTC report of the Specialist Committee on Cavitation and Erosion on Propellers and Appendages on High Powered/High Speed Ships.

Ligtelijn, *et al.* (2004) presented valuable results of a three-year research project, named CoCa (Correlation of Cavitation), in which correlation of propulsive performance, propeller

cavitation and propeller-induced hull-pressure fluctuations were studied. The focus of the project was on cavitation. Full scale experiments were carried out first, followed by model tests and computations in which the circumstances encountered on full scale were approximated as closely as possible. Five different ships used in this project are listed in Table 2.1. All model tests were performed in MARIN. Propulsion tests were conducted in the deep-water towing tank and the cavitation observations and hull-pressure pulse measurements in the depressurized towing tank. All the measurements are presented in normalized values.

Table 2.1 Ship type and propulsion system in CoCa project (Ligtelijn, *et al.*, 2004)

Ship's name	Ship type	Propulsion
P&O Nedlloyd Tasman	Containership 5,000TEU	Single FPP 54,900kW
P&O Nedlloyd Shackleton	Containership 6,800TEU	Single FPP 65,880kW
Costa Atlantica	Cruise ship	Twin Azipod 2x17,600kW
Amsterdam	Dredger	Twin CPP, Nozzle 2x7,000kW
Uilenspiegel	Dredger	Twin CPP, Nozzle 2x5,670kW

Although the level of correlation varied among different ships and test conditions, the speed-power correlations were in general satisfactory for all five ships, with the exception of the containership results in ballast condition. The speed-power relation for the cruise ship, Costa Atlantica, is shown in Figure 2.12 and the correlation between the prediction and trials appears to be very good.

The speed-power relations for container ship, Tasman for loaded and ballast conditions are shown in Figure 2.13. The agreement between prediction and trial is good for the loaded condition but not as good for the ballast condition. It should be noted that the runs in loaded condition were in Beaufort 6, but those in ballast condition were in better weather.

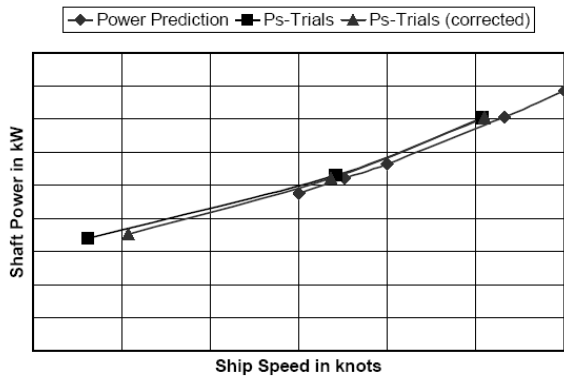


Figure 2.12 Speed-power correlation for cruise ship, Costa Atlantica (Ligtelijn, *et al.*, 2004).

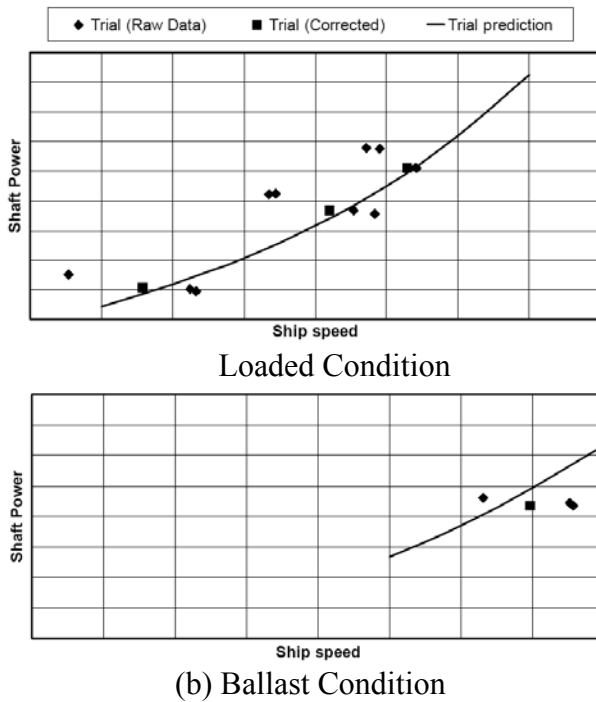


Figure 2.13 Speed-power correlation for container ship, Tasman, at loaded (upper) and ballast (lower) conditions (Ligtelijn, *et al.*, 2004).

For the pressure pulse level, the cruise ship with podded propulsion showed a good correlation as shown in Figure 2.14. The first blade-rate harmonic component of the fluctuating pressure in normalized form is presented in this figure. In case of the container ship, Tasman, pressure pulses at model scale were significantly higher than the full scale measurements as shown in Figure 2.15. The wake scaling effect is believed to be a dominant factor for

higher pressure pulses for model scale than that for full scale.

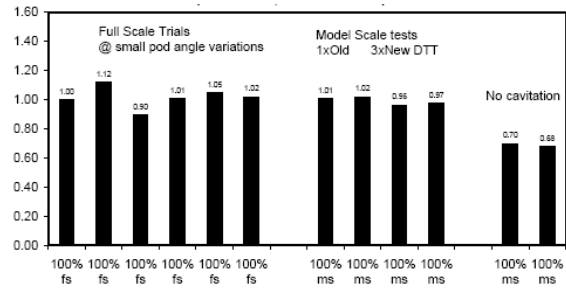


Figure 2.14 Hull-pressure fluctuations (1st blade rate) for cruise ship, Costa Atlantica, at 100% MCR (Ligtelijn, *et al.*, 2004).

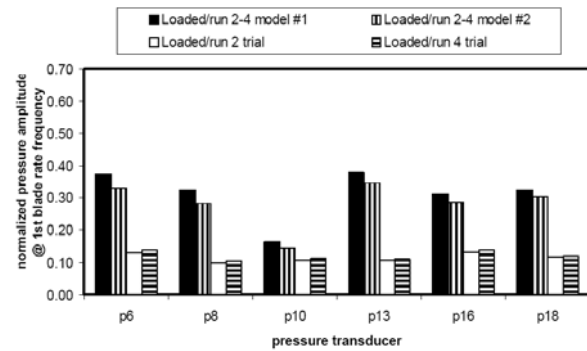


Figure 2.15 Hull-pressure fluctuations for container ship, Tasman at 100% MCR (Ligtelijn, *et al.*, 2004).

Bobanac, *et al.* (2005) developed a cost effective method for the observation and recording of full scale propeller cavitation (see Figures 2.16 and 2.17). The design enables relatively cheap and fast mounting/dismounting without necessity for expensive ship docking. The window with an optical prism, flat with the bottom plating, improves view angles without disturbing the ship wake.

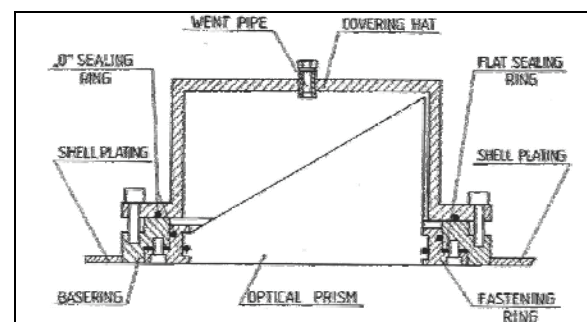


Figure 2.16 Cavitation observation window design (Bobanac, *et al.*, 2005).



Figure 2.17 Observation windows for twin-screw vessel (Bobanac, *et al.*, 2005).

Figure 2.18 compares the model and full-scale cavitation patterns for a small fast ship at two engine rpms (1,500 and 1,800). The authors concluded that cavitation patterns on model propellers did not correlate well with the full scale observations for a fast small ship.

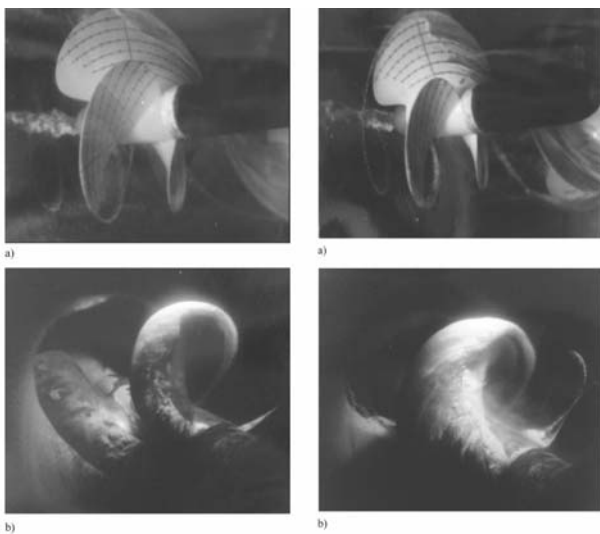


Figure 2.18 Comparison of model and full scale cavitation patterns for a fast small ship; LHS for 1500 rpm and RHS for 1800 rpm, (a) model (b) full scale (Bobanac, *et al.*, 2005).

Sampaio, *et al.* (2005) presented full scale trials for three different hull/propeller roughness conditions. The trials were performed with Brazilian patrol vessel ‘Guaporé’. The length and breadth of the vessel are 46.5m and 7.5m, respectively. Twin, three-bladed propellers of 1.44m diameter are installed. Nominal power of each shaft is 2,503hp at 642.5rpm. Ship trial conditions are summarized in Table 2.2.

Table 2.2 Trial conditions

Trial		I	II	III
Date (2001)		08/07	08/08	11/19
Draft, fwd	m	2.15	2.15	2.20
Draft, aft	m	1.95	1.95	1.95
Draft, mean	m	2.05	2.05	2.08
Displaced Vol.	m ³	272	272	276.8
Displacement	ton	278.3	278.3	283.3
Wetted Area	m ²	297.4	297.4	299.3

Trial I was carried out with the hull and propellers in fouled condition. For trial II, propellers were cleaned by a diver. Trial III was carried out just after a periodic maintenance docking. The full-scale tests consisted of a series of runs in calm seas without strong currents. During the test the propeller revolution was kept constant for a specific distance/time interval required for a constant advance speed. The reduction of power with the maintenance procedure is clearly seen in Figure 2.19. Although the hull surface condition was not described in the paper, it is clear that the fouling on hull and propeller surface greatly reduces the powering performance.

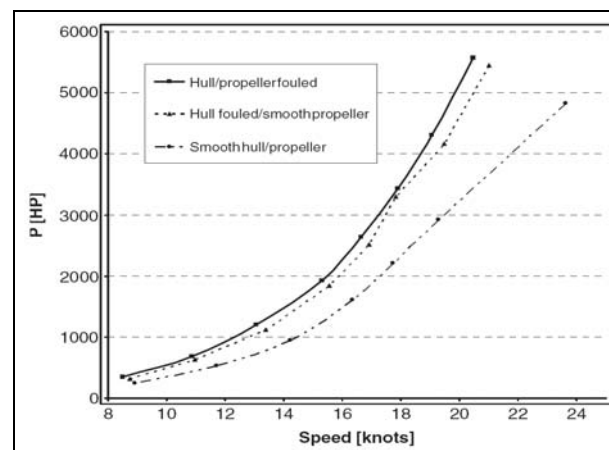


Figure 2.19 Comparison of speed-power for three different hull/propeller conditions (Sampaio, *et al.*, 2005).

2.2.5 Scale Effects: Tzabiras (2004) examined the scale effects on the resistance and propulsive characteristics of a ship using a steady-step procedure to calculate the free surface. A double-model, viscous-flow solver had been

extended to solve the free-surface problem employing a moving grid approach based on a conformal mapping technique which allows rapid grid adjustment under a specified boundary. The transport equations are solved according to a marching procedure based essentially on 2D computations. This is attainable due to the existence of the dominant velocity component parallel to ship axis as well as to the Dirichlet boundary condition for the pressure on the free-surface. The steady-state method has been applied successfully to solve the resistance and self-propulsion problems for a Series-60 $C_B=0.6$ hull at various Froude and Reynolds numbers. Calculated results for the integrated resistance and propulsion characteristics show satisfactory agreement with measurements at model scale. Computations at full scale demonstrate that the Froude hypothesis is valid.

Krasilnikov, *et al.* (2007) studied scale effects for ducted propeller performance using a RANS solver with a hybrid structured and unstructured grids for scale effects. The results indicated that when changing from model to full-scale conditions the duct thrust increased for all studied arrangements at all considered propeller loadings. The scale effect on duct thrust was more pronounced at lighter loadings where the relative contribution of viscosity was larger. It was also found that the blade area ratio of the propeller did not seem to have strong influence on increase in full-scale duct thrust. The change of full scale propeller thrust and torque compared to model scale was a complex, combined effect of the following factors: the increase in average flow velocity through the duct at higher Reynolds numbers; the decrease in thickness of the boundary layer on the interior duct surface resulting in different local blade loading at the tip and ultimately, to different flow picture around the blade tip and its effect on duct characteristics; and changes in both lift and drag of blade sections due to an increase in Reynolds number.

2.2.6 Self-Propulsion Predictions Using CFD The CFD Workshop Tokyo 2005 (Hino

Ed., 2005) provided a forum for computational analysts to evaluate the maturity of various CFD codes in predicting calm water resistance and self-propulsion performance of three hull-forms; container ship, VLCC, and naval combatant. Comparative computations of the flow characteristics for the KRISO container ship, KCS, without the rudder at self propulsion point were part of the workshop. The test conditions were $F_n = 0.26$ and $R_n = 1.4 \times 10^7$ at even keel (fixed trim and sinkage). Four groups participated in this category. They were Hamburg Ship Model Basin (HSVA), Potsdam Model Basin (SVA), KRISO (Korea Research Institute of Ships and Ocean Engineering, now MOERI, Korea) and Osaka Prefecture University (OPU).

Chao (2005) at HSVA used the commercial RANS code, COMET, for viscous flow computations using the RNG $k-\epsilon$ turbulence model with the standard wall function. He also used the potential-flow Quasi-Continuous Method (Lan, 1974) for the propeller flow. The propeller effect was computed using the body force concept with the actual propeller geometry taken into account. The body forces are distributed in the swept volume of the rotating propeller blades as functions of the axial, radial and tangential directions. The self-propulsion characteristics such as $(1-t)$ and $(1-w_t)$ were computed and compared with the experiments in Table 2.3. The predicted propeller torque in both open and behind conditions was higher than the measurements. Consequently the predicted open water efficiency (η_o), the relative rotative efficiency (η_r) and the quasi propulsive efficiency (η_D) are slightly lower than the measurement.

Lübke (2005) at SVA performed the self-propulsion simulation using the commercial code, CFX5. The sliding interface scheme was used to connect the rotating frame around the propeller and the fixed frame for the remaining part. The full propeller geometry was modeled in the computations yielding the transient interactions between ship and propeller for a self-propulsion simulation. Propeller and ship

alone were investigated for three different mesh configurations for grid convergence tests. For the simulation of self-propulsion, computations were performed only on the coarse (0.27M grid cells) and medium size meshes (2.15M grid cells) only. The self-propulsion characteristics are compared in Table 2.3. The propeller open water efficiency was significantly lower than the experiments. The thrust deduction factor ($1-t$) was higher and the wake fraction ($1-w_t$) was lower, thus giving a higher hull efficiency.

Kim, *et al.* (2005) at KRISO used their in-house RANS code, WAVIS for self propulsion simulation of KCS. WAVIS is a finite volume based multi-block RANS code. The realizable $k-\epsilon$ turbulence model with a wall function is employed for the turbulence closure. The free surface is captured with the two-phase level set method and body forces are used to model the effects of a propeller without resolving the detailed blade flow. The propeller forces are obtained using an unsteady lifting surface method based on potential flow theory. The self-propulsion point is obtained iteratively through balancing the propeller thrust, and the ship hull resistance. The unsteady lifting surface code is also iterated until the propeller induced velocity is converged in order to obtain the propeller force. The authors did not present the self-propulsion factors in their paper presented to the workshop, but presented them in a later paper (Kim, *et al.*, 2006). The numerical self-propulsion factors are in excellent agreement with experiment as shown in Table 2.3.

Tahara, *et al.* (2005) at OPU applied the RANS code, FLOWPACK, to their self-propulsion simulations. FLOWPACK code adapted a free surface tracking approach and is coupled with a propeller program (Nakatake, 1981) based on an infinite-blade propeller theory (Yamazaki, 1968). Propeller effects are included in the RANS equations by a thin body force approach. The body force distribution was iteratively determined by a propeller performance calculation based on the above-mentioned theory. Computational results of

the self-propulsion factors are in good agreements with experiments as shown in Table 2.3.

Hino (2006) at NMRI also calculated self-propulsion factors of KRISO Container Ship using the RANS code, SURF, developed in-house. A body force model is employed to take into account the propeller effect. The body force distributions are calculated using a simplified propeller model based on an infinite-blade propeller theory. The propeller open water performance predicted by the simple theory was satisfactory. The overall accuracy of the self-propulsion factors is good as compared with experiments in Table 2.3. Figure 2.20 shows the measured and computed axial velocity distribution behind a propeller. Although the computed accelerating flow is weaker than the measurements, general flow feature is well predicted. (*Note: In Hino's paper, the experimental and computational values of $(1-t)$ and $(1-w_t)$ were switched in his Table 7.*)

Table 2.3 Computational results of the self-propulsion factors
(Kim, *et al.*, 2006 and Hino, 2006).

	$1-t$	$1-w_t$	η_o	η_r	J	n rps	η
Exp.	0.853	0.792	0.682	1.011	0.728	9.50	0.740
HSVA	0.865	0.789	0.667	0.981	0.725	9.56	0.717
SVA	0.910	0.765	0.614	1.007	0.708	9.50	0.735
KRISO	0.846	0.779	0.671	1.023	0.729	9.38	0.746
OPU	0.852	0.789	0.631	1.074	0.718	9.53	0.732
NMRI	0.850	0.810	0.659	1.010	-	-	0.770
Mean	0.865	0.786	0.648	1.019	0.720	9.49	0.732
S.D.	0.026	0.016	0.025	0.034	0.009	0.08	0.020

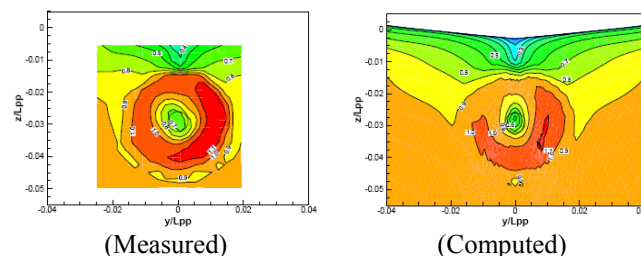


Figure 2.20 Comparison of measured and computed wake contours behind a propeller plane with propeller effect (Hino, 2006).

2.2.7 Propeller-Rudder-Hull Interactions:

Propeller-rudder and propeller-rudder-hull interactions are becoming increasingly important to further improve ship performance. Advancements in measurement techniques and computational capabilities enable the investigation of these complex interactions that affect ship performance.

Felli, *et al.* (2006) investigated the free-running propeller-rudder interaction with a focus on the tip vortex/rudder interaction. They used LDV phase sampling technique and high frame-rate CMOS camera to visualize the complex unsteady downstream flow details in the Italian Navy Cavitation Tunnel (CEIMM). For a computational method, they used an extended BEM method originally developed by Greco and Salvatore (2004).

An all-movable rudder with a simple rectangular planform with symmetric NACA 0020 profile and a four-bladed propeller with 0.272m diameter were used for the study (see Figure 2.21). The propeller was placed 0.4D ahead of the rudder. The rudder was placed off-center by 0.05m to the starboard side.

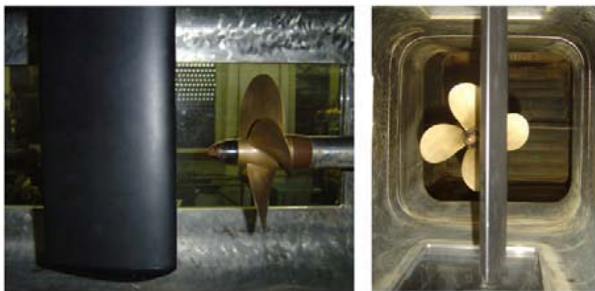


Figure 2.21 Overview of propeller-rudder installation (Felli, *et al.*, 2006).

Figure 2.22 shows the image of the propeller tip vortices along the rudder taken by a high-speed camera. The image shows details of tip vortex deformation as it moves along the rudder surface and eventually reconnects after passing the rudder trailing edge.

Takada, *et al.* (2002) developed a simulation method of free-surface flow around hull and

rudder with propeller effects using the RANS code, FS-MINTS, employing a multi-block grid technique. Propeller effects are included as body forces calculated by the unsteady Quasi-Continuous Method. Self-propulsion factors of a modern full ship with rudder are accurately estimated.

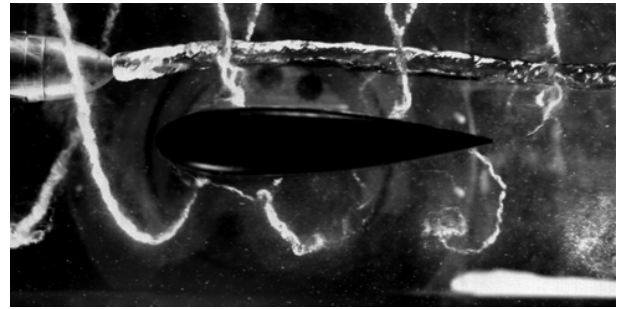


Figure 2.22 Chordwise evolution of propeller tip vortices at $t=0.0155$ sec (Felli, *et al.*, 2006).

Simonsen and Stern (2005) studied hull-propeller-rudder interaction with respect to ship manoeuvring using the RANS code, CFDSHIP-IOWA coupled with a simplified propeller model based on an infinite-blade theory. Computations are performed for an open-water propeller for the Series 60 ship sailing straight ahead and for the appended tanker Esso Osaka in different maneuvering conditions. The results are compared with experimental data, and the tanker data are further used to study the interaction among the propeller, hull, and rudder. A comparison between the calculated and measured data for the Series 60 ship shows a fair agreement, where the computation captures the trends in the flow. For the tanker, the flow study reveals a rather complex flow field in the stern region, where the velocity distribution and propeller loading reflect the flow changes caused by the different maneuvering conditions.

Kim, *et al.* (2007) investigated propeller-rudder-hull interactions for an LNG carrier model using experimental and computational approaches. They measured velocity fields at the propeller plane with and without rudder and propeller operations. The self-propulsion characteristics predicted by RANS code, WAVIS,

are in excellent agreement with experimental measurements. Detailed comparisons of computational results with experiments are presented in Section 4.2.

For high-speed ships, rudder cavitation is increasingly becoming an important maintenance issue. Paik, *et al.* (2008) investigated unsteady cavity patterns around the gap of the semi-spade rudders for a large container ship (see Figure 2.23). Several model-scale partial rudders with different thickness-to-chord ratios and gap sizes were investigated. Tests were conducted in the cavitation tunnel in a uniform flow without the propeller. The size of the partial rudder is 0.8 m (chord length at the mid-section) x 0.6 m (height) and the tunnel section size is 0.6 m x 0.6 m. Since the partial rudder occupies the entire tunnel height, blockage effects will be significant on the cavitation performance. Figure 2.24 shows a snapshot of unsteady gap cavitation for two different designs. They also measured the flow field using PIV and surface pressures using pressure tabs. However, their analyses and the presentation of the results were confusing. Correct interpretation of the results would require careful analysis of the data, including the effect of the tunnel blockage.

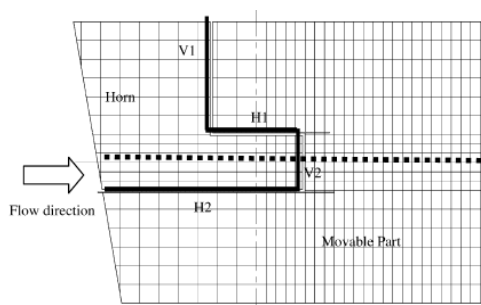


Figure 2.23 Partial model of a semi-spade rudder (chordlength = 0.8 m, height = 0.6m) (Paik, *et al.*, 2008).

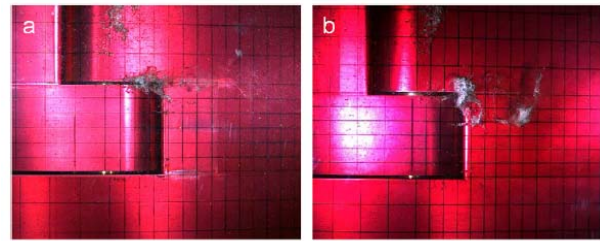


Figure 2.24 Snapshot of unsteady cavitation on partial rudders with different thickness ($\alpha=4^\circ$ and $\sigma=1.0$) (Paik, *et al.*, 2008).

2.2.8 Anti-Fouling Paint: In order to maintain the efficiency of a ship it is important to keep the propeller and the hull free from fouling. Current anti-fouling paints containing toxic components Tri Butyl Tin (TBT – SPC). International Maritime Organisation (IMO, 2001) and European Council and Parliament (EC) issued a regulation removing their use for ships completely by 2008 (EC, 2003). As a result, new environmentally friendly anti-fouling systems have been introduced to the market. Atlar, *et al.* (2005) reported that more than 150 full-scale propellers have been coated with such a paint type. Mutton, *et al.* (2005) reported that the coatings on the propeller surface of a research vessel, Bernicia, are almost intact after 37 months in service without cleaning. The roughness of propeller blade surface will affect the propeller efficiency. Atlar, *et al.* (2002, 2003) have calculated that a tanker propeller coated with foul release coating displayed a 6% gain in the efficiency of the same full-scale propeller without coating.

Korkut (2007) investigated experimentally the performance, cavitation and noise characteristics of a model tanker propeller in uniform flow and behind a simulated wake both with and without the coating. He showed that coating thickness on the model propeller is almost similar to that on full scale propellers and that particular care had to be taken with the trailing edge treatment to avoid singing. When applied correctly propeller performance was maintained. In order to quantify the effect of such coatings at model scale one should simulate the

surface roughness corresponding to in-service propellers.

2.3 Propeller Numerical Modelling

2.3.1 Bubble-Propeller Interaction: Hsiao, *et al.* (2006) developed a numerical model for gas diffusion across the bubble wall and incorporated in a multi-bubble dynamics code. The code was used to study bubble nuclei population dynamics in the propeller flow field that was obtained using a RANS solver. Bubble nuclei populations were propagated in this field. Large visible bubbles are seen to cluster in the tip vortices and in the wakes of the blades (see Figure 2.25). The bubble size becomes larger downstream of the propeller than the original upstream size due to a net influx of originally dissolved gas into the bubble. Bubble explosive growth and collapse, are an essential ‘catalyst’ to enable significant diffusion.

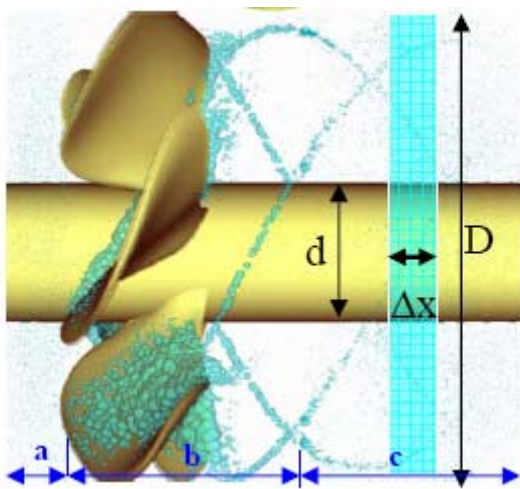


Figure 2.25. Bubble entrainment in the low pressure regions. Bubble sizes are to scale in section (b), They are enhanced by a factor of 5 in sections (a) and (c) (Hsiao, *et al.*, 2006).

In conjunction with microbubble drag reduction efforts in Japan, Kawamura, *et al.* (2007) investigated the effects of bubbles on the propeller efficiency. A two-fluid multiphase flow model was developed with the governing equations including the mass and momentum conservation of the mixture and the bubble phases. The validation of model was carried out using

experimental data for a 2D hydrofoil. Figure 2.26 compares the numerical predictions with measured lift and drag coefficients. For a given angle of attack, experimental data showed that the lift is reduced and drag is increased with increasing void fraction. Although the magnitudes are significantly different, the trend was correctly predicted by the numerical model. It was shown that bubbles are relatively accelerated around the leading edge of a hydrofoil or a propeller blade, and that the acceleration of liquid is reduced due to the bubble acceleration. This effect lowers the peak of the negative pressure at the leading edge resulting in the decrease in the lift and the increase in the drag coefficients.

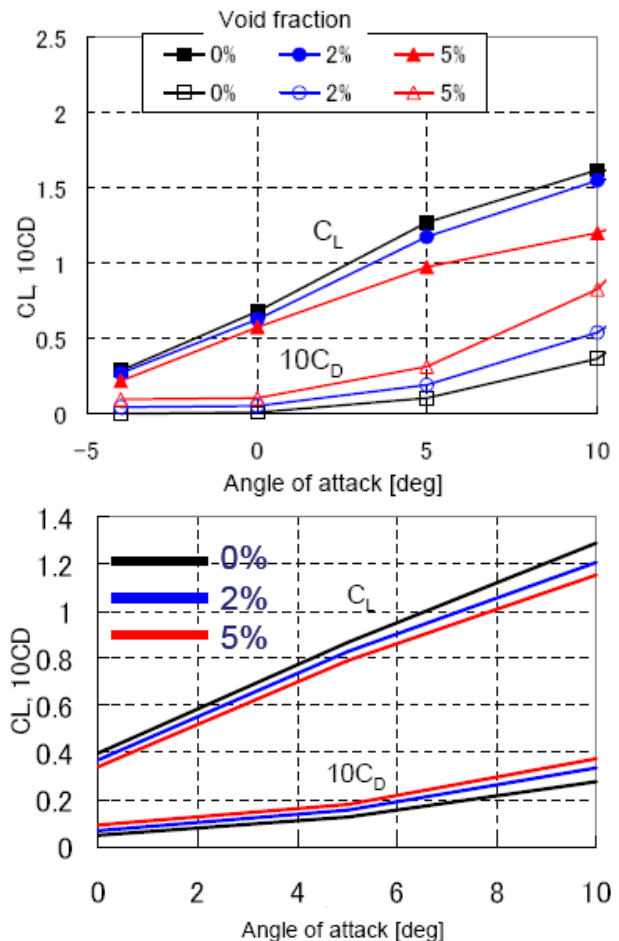


Figure 2.26 Measured (top) and computed (bottom) lift and drag coefficients of NACA 4412 foil section in single phase and bubbly flows (Kawamura, *et al.*, 2007).

The same numerical model was applied to the prediction of the propeller open water efficiency in bubbly flow. As shown in Figure 2.27, the efficiency decreases with increasing void fraction. The numerical predictions showed the same trend, but for a given void fraction, the numerical model significantly under-predicted the efficiency when compared to the experiments. For improving the quantitative accuracy it is probably necessary to include the effect of bubbles on the boundary layer characteristics, which is not included in the present model. The sensitivity to the assumed bubble size must also be investigated in the future.

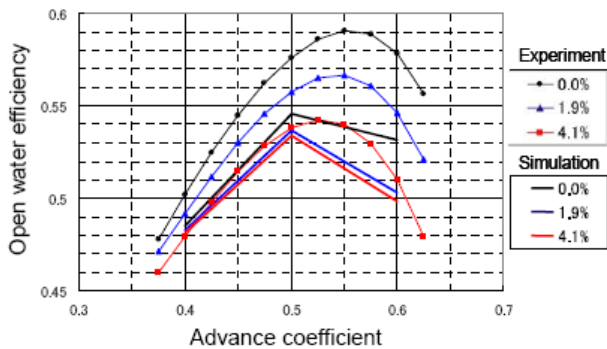


Figure 2.27 Measured and computed efficiency of the model propeller in single phase and bubbly flows (Kawamura, *et al.*, 2007).

The results of bubble effects on propeller performance may have a significant implication on the microbubble drag reduction efforts. The negative bubble effects on propeller performance should be minimized in order to achieve maximum net power reduction resulting from microbubble drag reduction.

2.3.2 Effects of Turbulence Model: Kawamura, *et al.* (2004) investigated the influence of the turbulence model on cavitating and non-cavitating propeller open water characteristics using the commercial RANS code FLUENT. Computations for a conventional propeller were carried out using a two-layer RNG $k-\epsilon$, standard $k-\omega$ and SST $k-\omega$ model. Thrust and torque coefficients were compared with measurements. The calculated torque coefficients were affected by turbulence model and the dis-

crepancy between calculated and measured torque coefficients was smallest in the case of the standard $k-\omega$ model.

Li, *et al.* (2006) studied the influence of turbulence model on the prediction of model- and full-scale propeller open water characteristics using RANS code, FLUENT. Three two-equation models, SST $k-\omega$, RNG $k-\epsilon$ and Realizable $k-\epsilon$ model were selected to study the scale effects of conventional and highly skewed propellers (see Figure 2.28). At model scale, the performance predicted by all the models is fairly close to each other. Compared to experiments, the prediction error is less than 2% for K_T and less than 12% for K_Q . For the conventional propeller at full scale, the performance predicted by the SST $k-\omega$ model differs marginally from the two $k-\epsilon$ models. For the skewed propeller at full scale, there is notable difference in performance. The SST model predicted that K_T is increased by about 5% with no change in K_Q . The $k-\epsilon$ models predicted slightly decreased K_T (~0.8%) and K_Q (~5-6%). The results suggest that the influence of turbulence model is dependent on propeller geometry.

An examination of the local skin friction distribution on blade sections revealed that only the SST $k-\omega$ model gives the expected distribution of local skin friction at both scales for both propellers. The $k-\epsilon$ models produce an erroneous skin friction for both propellers at full scale. Careful study is required to explain the doubtful results.

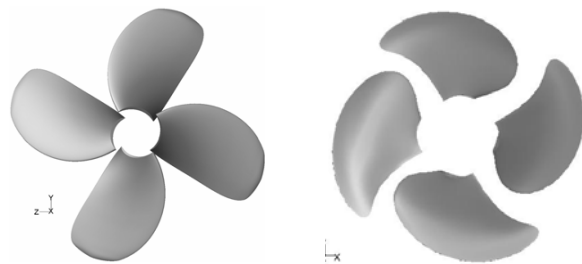


Figure 2.28 Conventional and highly-skewed propellers for RANS computations (Li, *et al.*, 2006).

2.3.3 LES for Complex Flow: Several papers presented applications of Large Eddy Simulation (LES) for steady and unsteady propeller flows. Bensow, *et al.* (2006) computed the propeller near-wake flow using LES on a rotating grid. The results were compared with PIV and LDV measurements. LES can provide useful qualitative information about the flow in the near wake concerning e.g. the evolution and interaction of tip and hub vortices with the blade.

Vysohlid and Mahesh (2006) successfully predicted highly unsteady, separated flow around a propeller in crashback operation using unstructured LES in a rotating frame of reference. Crashback is an operational mode where ship is moving forward but propeller is turning backward (negative rotation). Therefore, the sharp trailing edge of the blade becomes the leading edge, thus creating a large separated flow at the leading edge. Furthermore, the propeller is pushing the flow forward against the onset flow, creating a huge unsteady ring vortex around the propeller. Vysohlid and Mahesh successfully computed, arguably this most complex of propeller flows, using LES (see Figure 2.29). Previous attempts to compute the crashback flow using unsteady RANS code were not successful. It is likely that RANS is unable to adequately predict crashback because of the pervasiveness of large-scale unsteadiness.

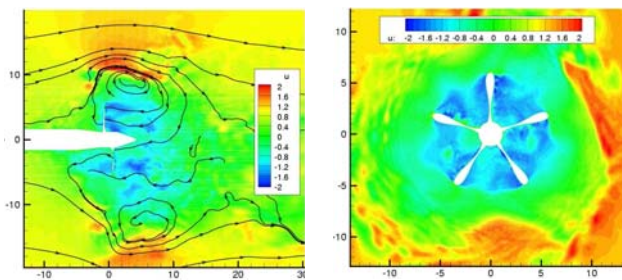


Figure 2.29 Contours of axial velocity and streamlines for crashback $J = -0.7$, $Re = 480,000$ (Vysohlid and Mahesh, 2006).

The mean values, root mean square (RMS) of velocity fluctuations and spectra of thrust, torque and side-forces were in a good agreement with experiment. Table 2.4 shows a comparison of computed mean thrust, torque

and side forces with water tunnel experiments. It is to be noted that the agreement of the RMS values between LES computations and the measurements is remarkable.

Table 2.4 Comparison of mean and RMS values at $J = -0.7$ (Vysohlid and Mahesh, 2006)

	K_T	K_Q	K_{fy}	K_{fz}
Mean (LES)	-0.38	-0.072	0.004	-0.002
Mean (Exp.)	-0.33	-0.065	0.019	-0.006
RMS (LES)	0.067	0.012	0.061	0.057
RMS (Exp.)	0.060	0.011	0.064	0.068

3. REVIEW ITTC RECOMMENDED PROCEDURES

- 7.5-01-02-01: Terminology and Nomenclature of Propeller Geometry (Harmonize with ISO standard)
 - 7.5-02-03-01.1: Propulsion Test
 - 7.5-02-03-02.1: Propeller Open Water Test
 - 7.5-02-03-02.3: Guide for Use of LDV
 - 7.5-02-05-02: High Speed Marine Vehicles Propulsion Test.
- (a) Determine if any changes are needed in the light of current practice.
 - (b) In the review and update of the existing propeller open water test procedure 7.5-02-03-02.1 its applicability to new types of propulsors should be taken into account.
 - (c) Identify the requirements for new procedures.
 - (d) Support the Specialist Committee on Uncertainty Analysis in reviewing the procedures handling uncertainty analysis.

3.1 7.5-01-02-01: Terminology and Nomenclature of Propeller Geometry

3.1.1 Review of Terminology: The Propulsion Committee reviewed the terminology and nomenclature of propeller geometry described in the ITTC document 7.5-01-02-01. In general, the document presented an extensive list of terminologies and nomenclatures for propeller geometry with clear explanations. However, minor but important changes and clarifications in the definition of some terms were recommended in a separate report submitted to the ITTC Advisory Council.

The Propulsion Committee also reviewed the ISO Standard described in the document BS EN ISO 3715-1: 2004 entitled *Ships and marine technology — Propulsion plants for ships — Part 1: Vocabulary for geometry of propellers*. This document was adopted as European and British Standards. In general, the vocabulary used for propeller geometry is defined well. However, there is a philosophical difference between the two documents. The propeller vocabulary in the ISO Standard is written from a manufacturing view point whereas the ITTC definitions are written from a hydrodynamic view point.

Careful comparison of the terminology for propeller geometry in the two documents revealed some differences in the definition of terms. For example, in the ISO Standard, several definitions of pitch were presented such as *pitch of pressure side, pitch of mean line, local pitch, pitch of mean line at leading point of blade section, pitch of mean line at trailing point of blade section, mean pitch of blade, mean pitch of propeller, and pitch at a certain radius*. The large number of pitch definitions does not appear to add significant value to manufacturers nor to towing tank researchers. Two definitions in the ITTC document, i.e. the geometric pitch and hydrodynamic pitch, appear to be sufficient for the ITTC community.

The definitions of skew and rake in the ISO document (Figure 7 of the ISO document) are not as rigorous as the ITTC definition. In the ITTC terminology, the *total rake* is defined as the sum of the (*pure*) rake and the *skew-induced rake*. The ISO document does not separate the two components. The *rake of blade sections* in the ISO is equivalent to the *total rake* in the ITTC terminology.

While several terminologies in both documents were related to the *expanded cylindrical blade section* (for example, the nose-tail line (chord line), camber (mean line), leading and trailing edges and the thickness), neither gave any explanation about how the blade section geometry is defined, particularly in the hydrodynamically important leading edge area.

There are two ways of defining the cylindrical blade section geometric characteristics in the expanded plane that are widely accepted by the propeller community. One way is to add the thickness to the chord line as shown in Figure 3.1 and the other is to add the thickness perpendicular to the mean line as shown in Figure 3.2 (Abbott and von Doenhoff, 1959). It was recommended in a separate report to the Advisory Committee that these two figures be included in the new ITTC terminology document.

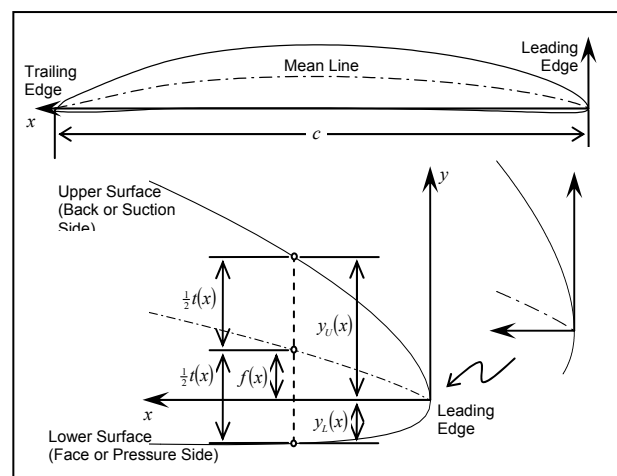


Figure 3.1 Definition of expanded cylindrical blade section geometry with thickness added normal to chord line (nose-tail line).

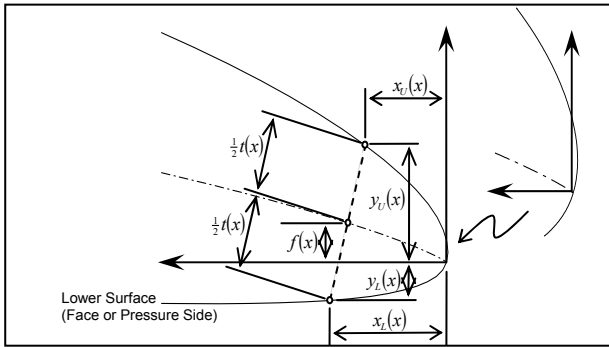


Figure 3.2 Definition of expanded cylindrical blade section geometry with thickness added normal to mean line.

3.1.2 Propeller Geometry Definition on Non-Cylindrical Sections:

For propellers with a highly tapered hub such as podded propulsor or a tip boundary such as ducted propulsor, the conventional method of describing their geometry in cylindrical sections is not adequate. Neely (1997) presented various methods for describing the propeller geometry based on non-cylindrical sections with the coordinate system shown in Figure 3.3. He derived equations for three non-cylindrical methods; a constant pitch angle method, a method based on geodesic curves, and a constant-pitch method. Each method has a characteristic equation that defines the nose-tail line and offset curves:

Constant Pitch Method: $r \tan \phi = \text{constant}$

Constant Pitch Angle Method: $\phi = \text{constant}$

Geodesic Method: $r \cos \phi = \text{constant}$

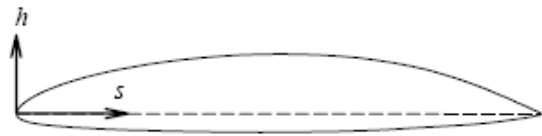
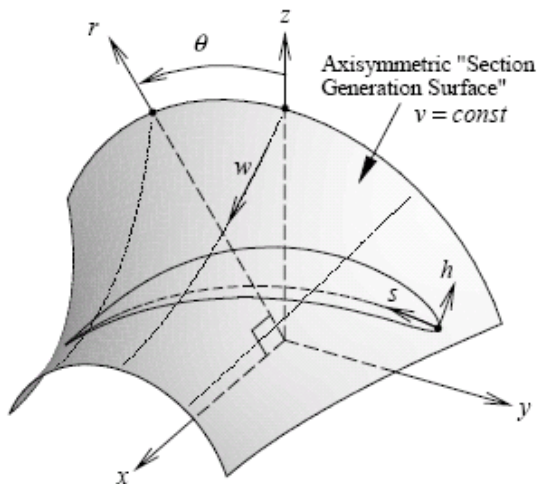


Figure 3.3 Coordinate systems for non-cylindrical sections (Neely, 1997).

While each method produced the identical result for the special case of cylindrical sections, each produced a significantly different result (see Figure 3.4), given the same basic input (pitch, camber, chord, thickness, skew and rake). He recommended that the constant-pitch-angle method be used for defining the propeller geometry on non-cylindrical sections since it was the simplest of the three, particularly in the special case of conical sections.

3.1.3 NURBS Surface for Propeller Geometry:

Numerically-controlled (NC) machines are increasingly used for fabrication of model-scale as well as full-scale propellers. Typically, a propeller design is passed to the manufacturer as a discrete set of x-y-z coordinates. The manufacturer must then interpolate the point set in order to define the NC tool paths in between the given points. The designer and manufacturer may have different surface definitions. As a result, the quality of the machined surface may not be what the designer intended. In order to avoid these types of problems, a common interpolation function is required. Then, the surface would be completely and uniquely defined, and anyone who uses the geometry would interpret it in exactly the same manner.

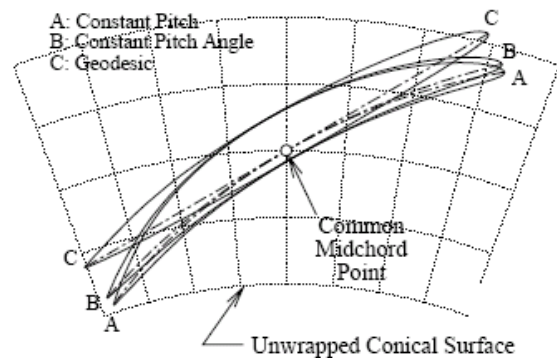


Figure 3.4 Sections generated from the same propeller parameters (Neely, 1997).

The Non-Uniform Rational B-Spline (NURBS) surface definition (e.g. Rogers & Adams (1990) and Farin (1990)) is widely accepted as the standard spline functions in the automobile, aerospace and shipbuilding industry. Neely (1998) presented an application of NURBS surface for defining the marine propeller geometry. Many commercial CAD software have the ability to generate NURBS surfaces given discrete data points.

Neely (1998) also provided techniques that would help to avoid common problems in generating propeller surfaces. Various parameterization schemes were discussed with regard to their effect on fitting a curve through points representing the foil geometry. A “half-cosine” parameterization scheme was introduced which is appropriate for airfoil or propeller blade section geometry. Its effect is to stretch out the leading edge region in parameter space, which results in a smooth curvature variation around the leading edge.

3.2 7.5-02-03-01.1: Propulsion Test

3.2.1 Propulsion Test Procedure Review:

The survey results by the 24th ITTC Propulsion Committee showed that the majority (79%) of the participating tow tank community did not think major changes were required in the Propulsion Test procedure. However, the procedure as written is quite general and leaves room for specific interpretations subject to individual tank’s routine practices, instrumentation equipment and model/full scale correlation procedures adopted. The Propulsion Test procedure review was accomplished in two aspects; minor editorial changes and suggestions for inclusion of special propulsion cases, not addressed in the current procedure.

3.2.2 Editorial Changes: In Section 1 Purpose of Procedure, the third paragraph from top: remove cycloidal propellers and paddle wheels, as these are not typical propulsion systems and seldom subject to self-propulsion testing. Include multi-screw propulsion systems

with split (different) power/RPM distribution among various propellers. Typically these may represent hybrid propulsion systems, double ended ferries, and multiple screw systems with propellers of variable diameter/pitch settings.

In Section 2.2 Definition of Variables: Add:

Nozzle Thrust	(N)	T_N
Thruster/Pod Unit Thrust	(N)	T_U
Thruster/Pod Unit Side Force	(N)	Y_U
Relative Rotative Efficiency	(-)	η_R

In Section 3.1.1.1 Hull Model: Add at the end of second paragraph “as well as thruster/pod unit thrust and side force”.

In Section 3.1.2.2 Propeller/Propulsion Unit Model: Add: “It is strongly recommended to couple the thruster and especially pod units to a steering machine, allowing step-wise rudder angle variation. Thus the optimum (minimum shaft power) unit rudder angle determination and adequate measurement of the unit side force could be efficiently executed. Additionally this set-up would allow dynamic pod loads measurements during model steering”.

In Section 3.1.3 Measuring Systems: Add: “Pod unit side force”.

In Section 3.2.2 External Tow Force, at the end of the first paragraph: The tow force is a correction to the hull resistance due to difference in friction between ship and model. Therefore, it is considered more feasible to apply the towing force in line with resistance force, i.e. at L_{CB} and V_{CB} . Hence replace “in the line of the propeller shaft and at the L_{CB} ” with “applied at L_{CB} and V_{CB} ”.

In Section 3.2.5 Speed: “The speed of the model should be measured to within 0.1% of the maximum carriage speed or to within 3 mm/sec, whichever is smaller. For a typical carriage maximum speed of 8 m/sec, 0.1% is 8 mm/sec that is more than twice larger than 3 mm/sec. As most of the recent towing carriages have a maximum speed of more than 3 m/sec,



the reference to the carriage maximum speed is obsolete and it is recommended to specify the speed accuracy only up to 3 mm/sec.

In Section 3.3 Calibration: Include guidance for calibration of the nozzle strain gauge and pod unit thrust and side force balance.

In Section 3.4.4 Measured Quantities: Delete the second and third paragraphs, in line with the proposed removal of cycloidal propellers and paddle wheels.

In Section 3.4.5 Shaft Tare Test: Delete the last paragraph, in line with the proposed removal of cycloidal propellers and paddle wheels.

In Section 3.5 Data Reduction and Analysis: The recommended reduction of wake fraction and relative rotative efficiency is based on the thrust identity. Many experimental facilities use also torque identity approach or both. The majority of full-scale trial performance measurements include propeller torque only. For practical correlation purposes the torque identity approach seems equally feasible. Therefore, it is recommended to include both thrust and torque identities.

3.2.3 Special Propulsion Test Cases

(i) Hybrid Propulsion Systems As already commented in the 24th ITTC Propulsion Committee report, several hybrid (mixed) propulsor arrangements have recently been reported. The basic idea behind these innovative propulsion systems is to decrease the propeller loading, as well as to decrease the rotational losses by application of the contra-rotating propeller concept. Typically the hybrid propulsion systems consist of conventional single (or twin) propeller, combined with azipod(s). The latter could be located aside the conventional propeller, or behind it, to utilize the contra-rotating effect. Additional benefit of this concept is the improved manoeuvrability.

Minami and Kawanami (2005) and Kawanami, *et al.* (2005) presented an excellent

summary paper on the Japanese Eco-ship project. The CRP podded propulsor, which was one of the propulsion systems investigated, enabled very good manoeuvrability and flexible control system in ship operation as well as high propulsion efficiency.

Ukon, *et al.* (2006) reported the model test results of a combination of podded propulsion with different stern shapes of a 50000 DWT product carrier. Details of the pod open water, ship model resistance and self-propulsion test procedures were also presented. Two analysis approaches were presented: the entire pod unit is considered as a propulsor and is not included in the resistance test, so called “system-base method”; the strut-pod is considered as part of the ship hull (appendages). This was defined as “propeller-base method”. Extrapolating the required power from the self-propulsion test, the correction for Reynolds number effect on the podded propulsor drag should be made by estimating the resistance of the podded propulsor both in full and model scale. The self-propulsion test was performed by the system-base method using the resistance of the bare hull and lowering the podded propulsor load from the ship self-propulsion point based on the propeller-base method.

Van and Yoon (2002) presented model test equipment and techniques for a cable laying ship equipped with twin azimuthing thrusters as prime movers. Three extrapolation methods with different definitions of thrust and resistance were compared. The authors concluded that more justifiable scale effect corrections for the azimuthing thruster components (thruster leg, pod, nozzle) have to be formulated.

Model testing and full-scale performance prediction for podded propulsors and hybrid propulsion systems are difficult in itself, and test procedures and prediction methods are still under development by the current 25th ITTC Specialist Committees on Azimuthing Podded Propulsion.

Sasaki, *et al.* (2006) presented a model test procedures for a hybrid pod and conventional propellers as a CRP unit. The paper also included a summary of the results from the Joint Research Project originally initiated by ABB, Veikonheimo (2006). The project objectives were to compare experimental results, analysis and performance predictions of podded propulsors among major European towing tanks. The testing scope included unit open water test, propeller alone open water test, pod resistance tests and analysis. The same model propeller was tested in all basins, while each basin manufactured its own pod model. Each basin had a different method of scaling the pod drag from model to full scale. Surprisingly the open water test results for the propeller alone showed greatest differences between scaling techniques and torque coefficient variations. This benchmark project showed that more work should be done when the accuracy level of results within +/- 2% is reached. It was concluded that development of more harmonized methods between different basins to scale podded propulsion performance will give better results.

Sasaki, *et al.* (2006) also reported a summary of the questionnaire regarding podded and hybrid CRP propulsion initiated and conducted by 25th ITTC Specialist Committees on Azimuthing Podded Propulsion. More than 40 organizations responded to the questionnaire. To the question "How do you perform self-propulsion test for a podded propulsor? 76% consider the entire pod unit as a propulsor, while the rest 24% consider the pod unit (housing) as an appendage. Regarding the hybrid CRP podded propulsion, 67% responded that they use propeller open water boat for the forward propeller and podded propulsor unit for the aft propeller. 17% perform open water test in a cavitation tunnel and the rest 16% use other method.

Finally Sasaki, *et al.* (2006) reported the procedure for conducting open water and self-propulsion test with hybrid CRP propulsor units as adopted by NMRI. It was proposed to carry out open water test for the entire propul-

sion system (forward and aft propeller), the results of which were analysed as system thrust and torque coefficients;

$$K_{TT} = K_{TF} + K_{TA} + K_{TU} \quad \text{Total thrust coefficient}$$

$$K_{TP} = K_{TF} + K_{TA} \quad \text{Propeller thrust coefficient}$$

$$K_Q = K_{QF} + K_{QA} \quad \text{Torque coefficient}$$

where:

K_{TF} – forward propeller thrust coefficient

K_{TA} – aft propeller thrust coefficient

K_{TU} – pod unit thrust coefficient

K_{QF} – forward propeller torque coefficient

K_{QA} – aft propeller torque coefficient.

Using K_{TT} identity, propeller revolutions, $(1-w)$ and η_R were defined based on hybrid system curves behind hull and open water, and final performance prediction was accomplished.

A major problem for conducting and analysing open water test for hybrid propulsors is the flow non-uniformity in the propeller plane. To establish this, a series of open water tests was proposed by Sasaki, *et al.* (2006), including wake measurements in the propeller plane behind the propeller open water test boat. Furthermore, the wake tests were performed at three different speeds of advance, as well as three to four variable propeller revolutions. It was concluded that wake and wave originating from the forward propeller open water test boat could affect the mean velocity at the pod propulsor disc.

Despite these efforts, there are still no widely accepted standard test procedures and full-scale performance prediction methods currently available for these hybrid propulsors.

In order to take full potential advantages of these hybrid propulsor concepts, improved test procedures and powering prediction methods need to be developed. Systematic powering tests in the towing tank will be needed, to-



gether with computations using relevant CFD codes.

(ii) Bollard Pull Test A large number of specialized ships, such as offshore supply vessels, cable laying vessels, salvage and stand-by platform support vessels, escort and harbour tug boats, fishing trawlers, etc. are typically equipped with usually ducted thrusters. Their operational profile very often requires bollard/trawl mode of operation, characterized with zero or very low speed of advance. Therefore, an accurate prediction of bollard/trawl pull performance is of equal importance with the propulsive performance prediction at speed.

Typically the bollard pull test is conducted as a part of the self-propulsion test, as the ship model, propulsion system, measuring equipment and instrumentation are usually the same as those for the self-propulsion test. However, the bollard pull test can be distinguished from the ordinary self-propulsion test by a few major differences:

- a) The bollard pull test is performed at variable propeller revolutions, covering a specified range of the engine power, typically from 50% to 100% MCR. This implies that the model propeller operates at different R_n , varying proportionally to the required variation of engine power (torque).
- b) The concepts of wake and relative rotative efficiency are no longer applicable in bollard pull condition, whereas the interaction with the hull is accounted for by the thrust deduction factor in the same manner as for the self-propulsion test. This also implies that propeller/or thrusters/pod unit open water characteristics are not necessarily required for the analysis.
- c) At bollard pull condition, the propeller induces very high axial velocities and acts as an axial pump. The flow through propeller disc is accelerated and creates

a current in the towing tank, depending on the tank's dimensions and the longitudinal position of the ship model relative to the tank length.

- d) At some conditions with very high loading, the propeller blades may start to ventilate due to air suction from free surface. This will significantly affect thrust and torque measurements. Furthermore, possible propeller cavitation and its influence on bollard pull performance cannot be modelled in a standard atmospheric pressure tank.

The bollard pull testing procedure needs to be addressed separately (or as a specific part of the self-propulsion test procedure), with special emphasis on the peculiarities outlined in items a) – d) above.

A series of performance and wake measurement tests were carried out in the Institute for Ocean Technology (IOT) towing tank in Canada and INSEAN large cavitation tunnel in Italy (Lababidy, *et al.*, 2006). In the performance tests, both the propeller and the duct thrust were measured at propeller geometric pitch ratio of 1.2 and at different propeller revolutions (15, 20 and 30 rps.). In the wake measurements, the flow characteristics were investigated using a stereo PIV system for the dynamic positioning (DP) thruster model wake at planes close to the thruster ($X/D=0.3$ and 0.5) when operating with and without a nozzle at bollard pull ($J=0$) and near bollard pull ($J=0.4$ and 0.45). The measurements provide insight about the performance and wake characteristics of the DP thruster under various operating conditions including the bollard pull. Some details of flow measurements are presented in Section 7.4.

Propulsion efficiencies, both for free sailing ahead and for bollard pull (merit coefficient), are characterized by the propulsor open water characteristics. Different propulsors have different characteristics, distinguished by the slope of K_T and K_Q curves. In an elaborate study of steerable thrusters, Dang and Laheij

(2004) showed that while open and CRP propellers are characterized by almost constant K_T and K_Q slopes over the entire J range, the ducted propeller thrust and torque curves showed different characteristics, especially near the bollard pull conditions, where the thrust curve becomes steep, while the torque curve becomes flat. This indicates that the thrust at bollard condition is sensitive to underwater current/vessel speed and propeller rate of turn, while the propeller torque is quite insensitive.

Hoekstra (2006) and Zondervan, *et al.* (2006) presented a RANS-based analysis tool for ducted propeller systems in open water condition including bollard pull. The propeller model was represented as an actuator disc, while the duct maintained its true shape. Systematic numerical simulations at various Reynolds numbers indicated that the scale effect on the duct thrust was modest except for R_n below 5×10^4 , where the scale effect became rather severe. It was found that the scale effect on duct thrust was primarily due to changes in the lift force on the duct, and less for the drag force. It was concluded that no indications have as yet been found that open water model tests could be misleading in evaluating the performance of a ducted propeller system, provided they are carried out at duct Reynolds number (based on duct chord) above 5×10^4 .

3.2.4 Recommendations: The above examples illustrate and highlight some of the potential problems associated with bollard pull testing and full-scale bollard predictions. Therefore, it is recommended that the self-propulsion testing procedure be further extended to include the bollard pull testing for open, CRP and ducted propeller systems.

3.3 7.5-02-03-02.1: Propeller Open Water Test

3.3.1 Overview. The survey carried out by 24th ITTC Propulsion Committee on the open water test procedure also showed that the ma-

majority of the participants indicated that there was no need to update the existing procedure. In response to a question related to open water test at two Reynolds numbers recommended by the ITTC, 6 (32%) answered that they perform open water experiments at only one Reynolds number that is higher than 0.5 million. In response to the question about Uncertainty Analysis recommended by the ITTC for propulsion and open water tests, the majority (18 out of 19) responded that they do not perform an uncertainty analysis as recommended by the ITTC. Six responded that they do uncertainty analysis according to their own procedures that are simpler than recommended by the ITTC.

On revisiting the procedure it was decided that the open water testing in a cavitation tunnel be added to the current procedure together with some editorial changes.

3.3.2 Open Water Testing in Cavitation Tunnel The current procedure is written only for towing tank applications in mind. However, open water tests can also be carried out in the cavitation tunnel if the institution does not have a towing tank facility. The procedure should, therefore, be extended to cavitation tunnel applications. However, the open water test results in the cavitation tunnel should be analyzed carefully by properly accounting for the tunnel blockage effects.

In the cavitation tunnel, a propeller model is mounted on a drive shaft. A streamlined nose cap is mounted upstream of the propeller model. The nose cap should have sufficient length to ensure that the inflow over the propeller hub is parallel to the shaft (see Figure 3.5). The connection between the cap and the hub should be smooth and without a gap. The size and shape of the nose cap should be recorded. In some cases the nose length may be less than $1.5 D$ as long as the flow is parallel to the shaft axis. The choice of propeller diameter should be made such that scaling effects are avoided within the blockage constraints of a given cavitation tunnel. The dimensions of the test section should be included in the test report. Open



water tests should be carried out under atmospheric condition and significant blade cavitation should be avoided.

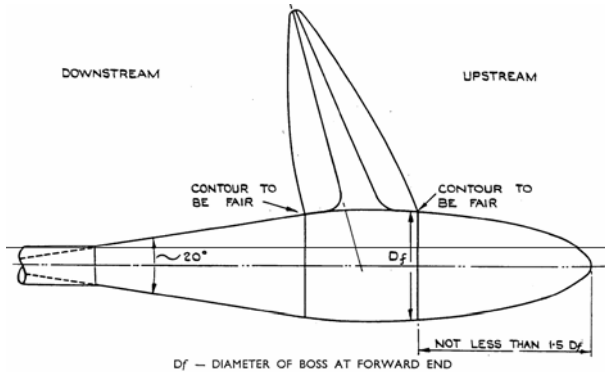


Figure 3.5 Typical model propeller geometry with a nose cap for open water testing (Figure 1 of the document, 7.5-02-03-02.1).

3.3.3 Editorial Changes. In Section 1 Purpose of Procedure, a sentence is included in the third paragraph as; “Podded propulsor open water test procedure is described in the document, 7.5-02-03-01.3 Podded Propulsor Tests and Extrapolation.”

In Section 2.1 Data Reduction Equations, the definition of K_{TP} is changed from “Thrust Coefficient” in ducted propeller case is corrected as “Ducted Propeller Thrust Coefficient”. The Reynolds Number definition was incorrect. The correct definition is:

$$Rn = c_{0.7R}(V_A^2 + (0.7\pi nD)^2)^{1/2}/\nu. \quad (3.1)$$

The section number for Conventional Propellers was incorrect. It should be 3.1.2.1 instead of 3.4.1.1.

The Section 3.1.2.1, Conventional Propellers is divided into two subsections: 3.1.2.1.1 Towing Tank and 3.1.2.1.2 Cavitation Tunnel. A sentence is added to the end of the first paragraph. “In some cases the nose length may be less than 1.5 D as long as the flow is parallel” is added to the end of the first paragraph. The last sentence at the end of third paragraph is modified as “A typical set up for a towing tank is shown in Fig. 2.” The captions for Figures 2 and 3 are changed as: “Typical Set Up for Tests

on Conventional Propellers in a Towing Tank” and “Typical Set Up for Tests on Ducted Propellers in a Towing Tank”, respectively.

In Section 3.1.2.1, a new subsection “Cavitation Tunnel” and its content are added for the installation of propeller models to carry out open water tests in cavitation tunnels.

In the last sentence of the second paragraph in Section 3.1.2.2 Ducted Propellers is modified as, “A typical set up for a towing tank is shown in Fig. 3.” “Set-up for a cavitation tunnel is similar to the towing tank set-up” is added.

In Section 3.3.4 Rate of Revolution, the paragraph starting with “The measurement instrumentation ...” are written twice and one should be removed.

In Section 3.3.5 Speed, the paragraph is modified as; “The speed of the propeller model should be measured to within 0.1% of the maximum carriage speed or within 3 mm/sec, whichever is the larger for towing tanks. In the cavitation tunnel the speed should be measured within 1% of the maximum tunnel speed.”

In Section 3.4.5 Speed, the paragraph is modified as; “The calibration of the carriage or tunnel speed will depend mainly on how the speed is measured in each facility. The carriage and tunnel speed should be checked regularly and respective records should be stored.”

In Section 3.5 Test Procedure and Data Acquisition, the last paragraph is modified as “The propeller open water tests should be conducted at least at two Reynolds Numbers; one should be at the Reynolds Number used for the evaluation of the propulsion test, which should be higher than 2×10^5 and the other should be as high as possible.”

In Section 3.6 Data Reduction and Analysis, a sentence is included in the first paragraph as; “In the case of cavitation tunnel experiments, the measured velocity, thrust and torque values are corrected for tunnel wall effects, for exam-

ple, based on the work of Wood and Harris (1920). It should be noted that the key point is that an appropriate tunnel blockage correction is applied, notwithstanding the longevity of the quoted reference.

In Section 3.7 Documentation, the second bullet is modified as; “Particulars of the towing tank or cavitation tunnel, including length, breadth and water depth for towing tank, or test section length, breadth and height for cavitation tunnel”.

3.4 7.5-02-03-02.3: Guide for Use of LDV

Since the membership of the 25th Propulsion Committee did not have sufficient expertise in LDV to review the current LDV guidance, it was decided that the Committee would review major LDV papers recently published. As LDV is widely used in the cavitation tunnel and the towing tank for flow measurements around propellers and ship hulls. It is evident that there is an increased use of Particle Image Velocimetry (PIV) and this literature is included.

3.4.1 Recent Development: Michael and Chesnakas (2004) presented comprehensive LDV measurements of flow around a mixed-flow waterjet pump model (see Figure 3.6). The unit was placed inside a pod and in the open jet of the 36-inch water tunnel of DTMB. Windows in the pod allowed optical access for LDV measurements to be obtained at four stations: in the inlet section, in between the rotor blades, in between the rotor and stator, and at the nozzle exit. The windows were curved to match the inside profile of the pump, thus minimizing the flow disturbance. The thin, 0.76mm, windows ensured that the laser-beams would pass through the curved windows with minimal optical distortion. At the station between the rotor and the stator, the LDV system consisted of two optical probes to measure three components of velocity, i.e. the vertical, axial and cross-stream horizontal component. The measurements revealed some interesting

details of the pump flow. Blade wakes are clearly visible. A vortex can be seen close to the tip on the pressure side of the blade. The leakage vortex is formed by flow on the pressure side of the blade crossing through the tip gap to the suction side of the blade.

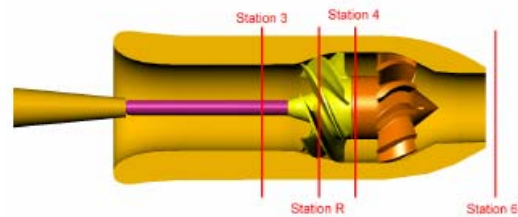


Figure 3.6 LDV measurement stations (Michael and Chesnakas, 2004).

Abdel-Maksoud, *et al.* (2004) investigated the influence of hub cap shape on propeller efficiency and cavitation inception. They carried out LDV measurements to analyze the difference in velocity field with different hub cap shapes. The measured results were used for CFD validation.

Felli, *et al.* (2006) measured the evolution of the propeller-rudder wake flow using LDV at different downstream locations. Figure 3.7 shows the measured axial velocity distribution downstream of the propeller at two longitudinal locations, ahead and behind the rudder. The effect of the rudder can be recognized by the defect of the axial velocity in both the upstream and downstream planes. The upstream deficit is caused by the flow blockage of the rudder that induces locally a slowdown of the slipstream, according to the authors and noted by Molland and Turnock (2007).

Figure 3.8 shows the evolution of the vorticity field upstream and downstream of the rudder. The spanwise distribution of shear of the tip vortices is not symmetrical and appears larger on the upward rotating propeller region.

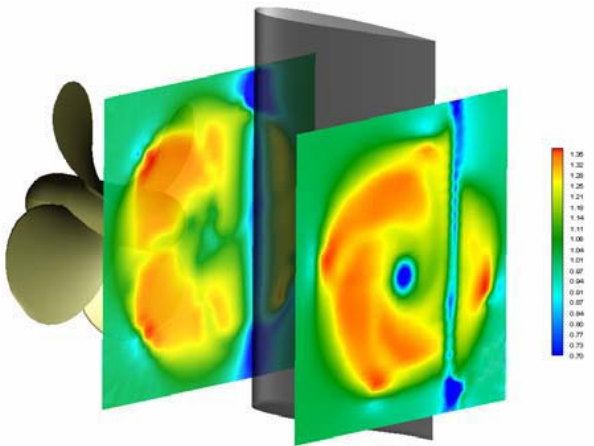


Figure 3.7 Evolution of the axial velocity upstream and downstream of the rudder (Felli, *et al.*, 2006).

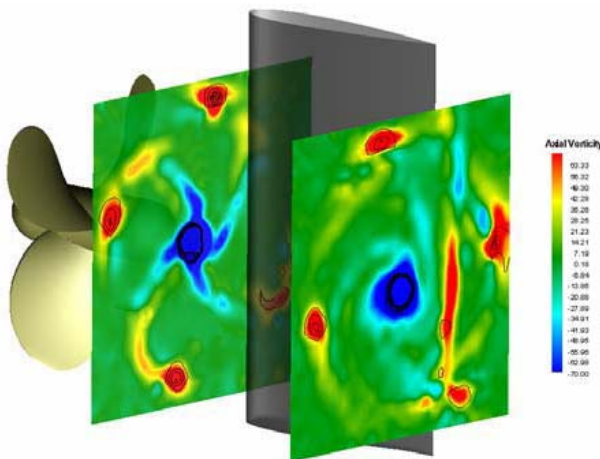


Figure 3.8 Evolution of the vorticity field upstream and downstream of the rudder (Felli, *et al.*, 2006).

Jessup, *et al.* (2004) investigated the performance of a conventional open propeller at extreme off-design conditions including near bollard and crashback conditions by using LDV and PIV techniques. Tests included measurements of load, cavitation observations and flow visualization. For crashback conditions, the recirculating ring vortex is documented (see Figure 3.9). Instantaneous PIV images show the unsteady movement of the ring vortex in and out of the propeller plane. The flow at the near bollard condition for the lowest J obtainable in the cavitation tunnel was investigated. The blade flow shows a significantly thicker blade wake than typically observed for

propellers operating at design J . Also seen is the intense tip vortex.

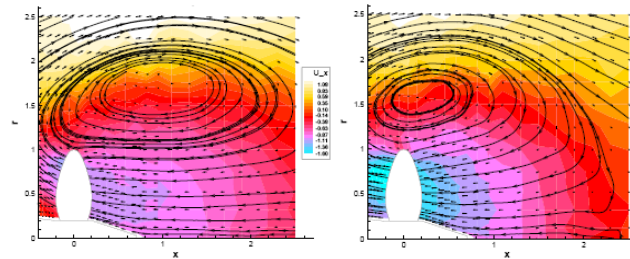


Figure 3.9 Time average axial velocity and streamlines for $J=0.7$ (left), $J=0.5$ (right) (Jessup, *et al.*, 2004).

Jessup, *et al.* (2006) continued their investigation of flow around a ducted propulsor in crashback operation using LDV and PIV. A more detailed review is presented in Section 4.3.

Atlar, *et al.* (2007) used LDV to measure propeller race at various stations downstream of the podded propulsor in the cavitation tunnel. Lübke and Mach (2004) used LDV to measure the wake of the propelled container ship, KCS, model.

Paik, *et al.* (2007) investigated the near-wake characteristics of a 4-bladed marine propeller model ($D=0.25$ m) in the cavitation tunnel using a PIV technique. The Reynolds number based on the chord length at 0.7 radius was about 3×10^5 . 150 instantaneous velocities were measured for each of 9 phase angles ($0 \leq \phi \leq 80$ deg.) of the propeller blade. The zero phase angle corresponds to the blade in the upright position. The instantaneous velocities were ensemble-averaged to obtain the spatial evolution of the tip and the trailing vortices of the propeller wake (see Figure 3.10).

Lababidy, *et al.* (2006) measured the wake flow of a ducted dynamic positioning thrusters in the INSEAN cavitation tunnel using a stereo PIV system. This paper is reviewed in more detail in Section 7.4.

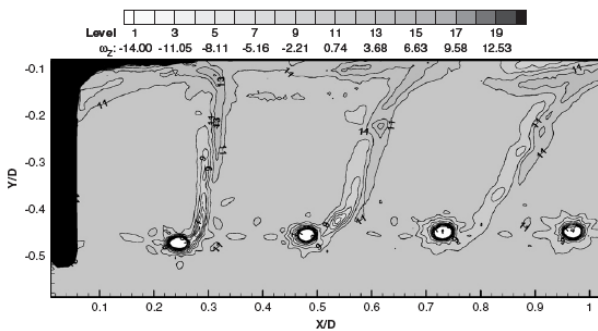


Figure 3.10 Phase-averaged vorticity in the longitudinal plane at $\phi = 10$ deg. (Paik, *et al.*, 2007).

3.4.2 Recommendations: The LDV technique is widely used to investigate detailed flow characteristics around propeller. The PIV is also becoming popular for measuring complex ship and propeller wake flow. Several important papers were presented for tip vortex and crashback flow investigations. It is recommended that a Specialist Committee be established to thoroughly evaluate the recent efforts and come up with guidelines for the next ITTC conference.

3.5 7.5-02-05-02: High Speed Marine Vehicles Propulsion Test

The Propulsion Committee reviewed the existing procedure and made a number of changes to ensure compatibility of the terminology with 7.5-02-05-02. In particular, the definition of what constitutes a high speed marine vehicle (HSMV) has been made the same.

A classification of the different types of HSMV is now included in the procedure. However, it should be noted that depending on the type of vessel and on the physical phenomenon used it is not possible to identify specific procedures for each vessel type. The procedure can now be considered to be a high speed propulsion test process which can be applied to a variety of vessel types. Waterjet powered vehicles are now explicitly excluded from this procedure.

It is acknowledged that the procedure is not yet complete. For instance the appropriate process for open water testing of inclined shaft propulsors will require considerable effort and would rely on the availability of good quality full scale data for validation of suitable scaling.

4. CRITICALLY REVIEW EXAMPLES OF VALIDATION OF PREDICTION TECHNIQUES. IDENTIFY AND SPECIFY REQUIREMENTS FOR NEW BENCHMARK DATA

4.1 Introduction

Two CFD workshops were recently held with the purpose of assessing the level of maturity of computational fluid dynamics codes in predictive capability of various hydrodynamic flows. One was the CFD Workshop Tokyo 2005 (Hino, Ed., 2005) where CFD capabilities were evaluated for calm water resistance and self-propulsion performance for several ship models. The other was the recent SIMMAN 2008 workshop held in Denmark where the participants evaluated the capabilities of CFD codes to make maneuvering predictions. Both Workshops presented well documented experimental data that could be used for validation of various CFD codes for resistance, self-propulsion and maneuvering performance in calm water with and without propellers.

Several other recent papers presented archival quality experimental data that can also be used for validation of CFD codes. Two papers are reviewed here. One presented detailed flow measurements at the stern of a fully-appended ship and self-propulsion factors at different conditions. Another paper presented the measurements of complex separated flow around a ducted propeller at crashback operations.



4.2 Hull-Propeller-Rudder Interactions

For the design of hull forms with better resistance and propulsive performance, it is essential to understand flow characteristics, such as wave and wake development, around a ship. Experimental data detailing the local flow characteristics are invaluable for the validation of the physical and numerical modeling of CFD codes, which are recently gaining attention as efficient tools for hull form evaluation.

Kim, *et al.* (2007) performed a numerical simulation of turbulent free surface flow around a self-propelled MOERI 138,000 m³ LNG Carrier (KLNG) with a rudder and a propeller. They used their in-house RANS code, WAVIS, with the overset grid scheme. They investigated numerically complex flow phenomena around the stern region due to propeller-hull-rudder interaction. Figure 4.1 shows a comparison of the computed and measured axial velocity at right behind the rudder at the self-propulsion condition. The agreement is good. Figure 4.2 presents a comparison of computed and measured streamlines on the rudder surface at self-propulsion condition. The computations captured the difference of the streamlines on both sides of the rudder very well. The computed self-propulsion characteristics such as thrust deduction, wake fraction, propeller efficiency, and hull efficiency with and without the rudder are also in good agreement with the experimental data as shown in Table 4.1. The effects of propeller and rudder on the ship wake and wave profiles in the stern region are clearly identified. The results contained in this paper can provide an opportunity to explore integrated flow phenomena around a model ship in the self-propelled condition, and can be added to the ITTC benchmark data for CFD validation as the previous KCS and KVLCC cases presented in the CFD Workshop Tokyo 2005.

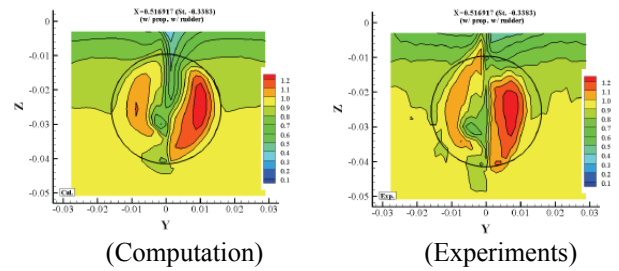


Figure 4.1 Comparison of axial velocity contours at self-propulsion condition with rudder (Kim, *et al.*, 2007)

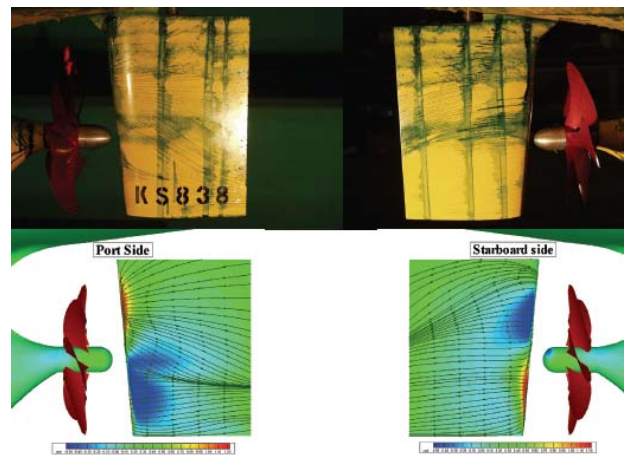


Figure 4.2 Comparison of paint streaks (upper) and computed streamline (lower) on rudder surface (Kim, *et al.*, 2007).

Table 4.1 Comparison of self-propulsion parameters for KLNG without and with rudder (Kim, *et al.*, 2007)

(Without Rudder)					
	K_T	$10K_Q$	$l-t$	$l-w$	η_H
Exp.	0.2244	0.335	0.745	0.628	1.186
Cal.	0.2254	0.342	0.779	0.607	1.283
	η_o	η_r	J	n	η_D
Exp.	0.6107	1.010	0.5788	7.96	0.732
Cal.	0.6121	1.003	0.5859	7.60	0.788
(With Rudder)					
	K_T	$10K_Q$	$l-t$	$l-w$	η_H
Exp.	0.2380	0.345	0.7500	0.584	1.284
Cal.	0.2364	0.353	0.7747	0.5797	1.336
	η_o	η_r	J	n	η_D
Exp.	0.5915	1.023	0.5521	7.76	0.777
Cal.	0.5977	1.006	0.5653	7.52	0.804

4.3 Crashback Flow around Propeller

Jessup, *et al.* (2006) continued their investigation of unsteady propeller performance in crashback conditions in the David Taylor Model Basin (DTMB) 36-inch water tunnel for an open and a ducted propeller (see Figure 4.3). The open propeller was the same one used for their previous crashback investigation (Jessup, *et al.*, 2004).

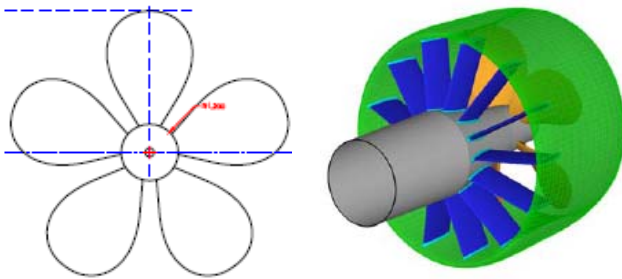


Figure 4.3 Propeller and duct configuration for crashback experiments (Jessup, *et al.*, 2006).

Tests were conducted with and without a duct. The unsteady flow was measured using Stereo Particle Image Velocimetry (SPIV) technique. Unsteady shaft loads and blade strains were also measured. The large recirculation ring vortex was measured along with inflow through the propeller disk (see Figure 4.4). The addition of a duct tends to move the ring vortex outboard, and maintains attached flow on the outer duct surface. This potentially could result in large duct side forces. They recently measured the duct forces that will be presented in the future. Measurements showed the cross flow through the propeller disk correlated well with the measured unsteady side forces. Peak blade strain was measured to be significantly larger than previously documented measurements. Peak strains of 3.5 times mean strain were measured as compared to previous factors used of 1.65.

The PIV data collected previously on open propeller crashback testing (Jessup, *et al.*, 2004) and those presented here for ducted propulsor (Jessup, *et al.*, 2006) are contained within a database which can be made available upon

request. These data would be valuable information for validation of computational codes for predicting highly unsteady crashback flow.

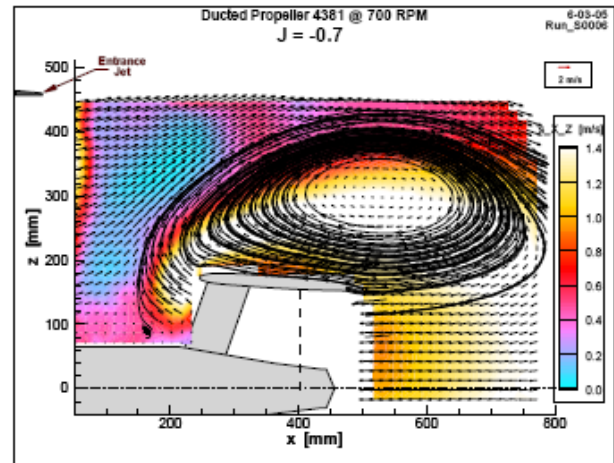


Figure 4.4 Time-average velocity showing a large ring vortex outside the duct (Jessup, *et al.*, 2006).

4.4 Recommendation

The archival-quality experimental data described above can be added to the ITTC benchmark data for CFD validation. They are (1) KRISO containership, KCS, self-propulsion test data presented to the CFD Workshop Tokyo 2005 (Hino, Ed., 2005), (2) the multi-partner collaborative ship maneuvering test data presented to the SIMMAN 2008 Workshop and further reported on in the 25th ITTC Manoeuvring Committee report, (3) hull-propeller-rudder interaction test data on MOERI 138K LNG Carrier (KLNG) (Kim, *et al.*, 2007), and (4) PIV data for unsteady flow around open propeller (Jessup, *et al.*, 2004) and ducted propeller at crashback conditions (Jessup, *et al.*, 2006).



5. REVIEW THE DEVELOPMENT AND PROGRESS IN UNCONVENTIONAL PROPULSORS SUCH AS TIP-RAKE, TRANS-CAVITATING AND COMPOSITE PROPELLERS (HYDROELASTICITY AND CAVITATION EROSION SUSCEPTIBILITY TAKEN INTO ACCOUNT)

5.1 Introduction

Previous Committees have carried out reviews of unconventional propulsors. The 21st Propulsor Committee (1996) reviewed contra-rotating propellers, propeller with a vane wheel, end plate propeller, podded propulsor, boss cap fin, pre-swirl stator, ducted propeller and ring propeller. The Specialist Committee on Unconventional Propulsors of the 22nd ITTC (1999) reviewed and evaluated propulsion tests and extrapolation methods for these unconventional propulsors. The 23rd Propulsor Committee (2002) reviewed composite propellers. The 24th Propulsor Committee (2005) gave an overview of waterjets, podded propulsors, tip plate propellers, rim-driven propellers, trans-cavitating propellers and composite propellers.

The present Committee reviewed and presented below only the recent progress in these unconventional propellers, together with some new concepts.

5.2 Tip-Rake/Plate Propeller

Sánchez-Caja, *et al.* (2006a) computed the flow around the endplate propeller by using RANS solver FINFLO at model and full scale. Good correlations with model scale experiments were obtained in terms of force coefficients. Some flow features were computed, including the leading edge vortex typical of skewed blades and the vortex at the outer region of the endplate. Figure 5.1 shows the pressure distributions over the suction side of both model and full scale blades. Figure 5.2 shows

the in-plane velocity vectors in the near wake of the endplate. It shows the endplate tip-vortex is stronger at full scale. Their calculations showed a larger scale effect on the thrust coefficient (almost 10 percent) than that found for conventional propellers (see Table 5.1).

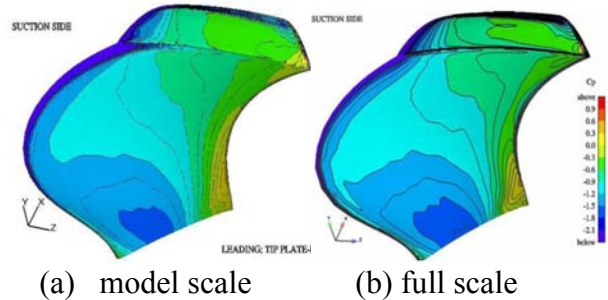


Figure 5.1 Calculated pressure distributions over suction side of end-plate propeller (Sánchez-Caja, *et al.*, 2006a).

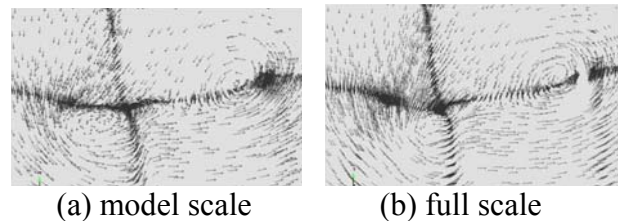


Figure 5.2 In-plane velocity vectors on near wake of the endplate (Sánchez-Caja, *et al.*, 2006a).

Table 5.1 Scale effect on performance coefficients (J=0.78) (Sánchez-Caja, *et al.*, 2006a)

	Calculations, normalised by model scale values	
	Model scale %	Full-scale %
K_T	100	109.7
K_Q	100	103.6
η_0	100	105.9

Chen, C.T. *et al.* (2006) proposed a special kind of tip modified propeller, named as a tip-fillet propeller (see Figure 5.3). The tip fillet was defined by several geometric parameters; maximum thickness at tip, chord length and camber of tip section and the start point of the

fillet in the radial position. Several cases were examined using a boundary element method and a RANS solver. The authors found that the maximum thickness at the tip and the fillet starting point have a significant effect on propeller efficiency, while the chord length and camber of the tip section have a major influence on the tip vortex cavitation. The efficiency of a symmetric tip-fillet propeller is higher than that of an asymmetric design, while an asymmetric tip-fillet propeller is more effective at controlling the tip vortex. Experimental comparisons with a conventional propeller are planned in the near future.

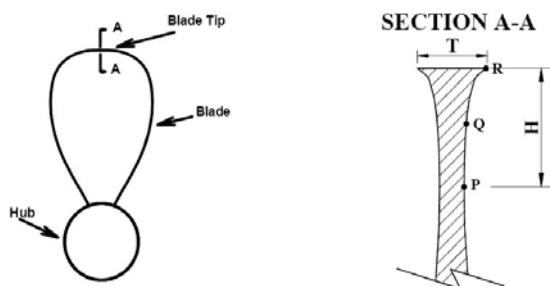


Figure 5.3 The sketch of tip-fillet propeller (Chen, C.T. *et al.*, 2006).

Yamasaki and Okazaki (2005) designed a straight leading edge propeller (SLEP) and a backward tip rake propeller (BTRP) for a container ship and conducted an open water test, the observation of cavitation and the measurement of the pressure fluctuations. The propeller open water efficiency of SLEP was better than that of a standard propeller and the pressure fluctuations of BTRP were lower than those of the standard propeller. For both propellers the blade surface cloudy sheet cavitation was connected to tip vortex cavitation. The risk of the cavitation erosion was confirmed around the trailing edge at 0.9R of BTRP.

Yamasaki and Okazaki (2007) designed a new BTRP for a low speed ship of which the pressure fluctuations (2nd blade frequency) was high. The new BTRP was designed such that the blade surface changing due to a rake was smoother than that of previous BTRP in order to avoid the cavitation erosion. Model tests confirmed that the propeller open water

efficiency of the new BTRP was comparable to that of a standard propeller and the pressure fluctuations (2nd blade frequency) of the new BTRP was reduced by about 51% compared with a standard propeller without the risk of the cavitation erosion due to the new rake distribution.

Kuiper, *et al.* (2006) proposed propeller design techniques to delay the tip vortex cavitation inception. Important parameters in the tip region including thickness, planform, skew, chord distribution and rake were systematically varied while maintaining a constant radial loading distribution. A systematic series of 2-bladed propeller designs was evaluated using a panel method for pressure distribution near the tip. An extreme tip rake towards the pressure side was used in the investigation as shown in Figure 5.4. The measurements showed a trailing vortex coming from the corner of the raked tip. There was still too much cross-flow over the area of strong curvature, leading to separation and vortex formation. Local and leading edge tip vortex inception were delayed significantly, while the width of cavitation bucket for the trailing tip vortex inception was reduced moderately. The authors believe that the strong curvature in the tip region should be avoided and rake with a smoother curvature (right-side of Figure 5.4) may be preferred, as used in authors' previous work (Kuiper, 1994).

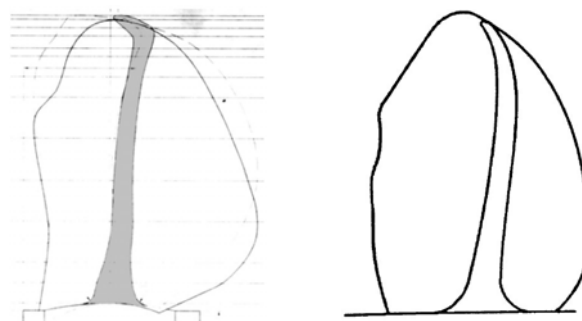


Figure 5.4 Tip rake with a strong curvature (left) and a smooth curvature (right) (Kuiper, *et al.*, 2006).

5.3 Surface-Piercing Propeller (SPP) and Super-Cavitating Propeller (SCP)

Young (2004) presented a coupled BEM/FEM approach to compute the time-dependent hydroelastic response of SPPs. The hydrodynamic part of the analysis is performed using a BEM, which was reviewed in detail in the 23rd and 24th ITTC Propulsion Committees. To account for the fluid-structure interaction, two hydroelastic models were used. The first model couples a BEM with an FEM, and in the second model the blade is simplified as a single degree-of-freedom (SDOF) system. The predicted natural frequencies as a function of blade angle using the BEM/FEM approach compared well with experimental measurements. The predicted time-dependent axial force coefficient using the BEM/SDOF approach also compared well with experimental measurements. There are some discrepancies at the blade entry and exit phase for cases with a low advance coefficient due to the effects of jet sprays, and rise in overall free surface elevation. The author suggested that the BEM model need to be improved to account for nonlinear free surface effects.

Nozawa and Takayama (2005) presented a method to compute the running attitude of the high speed craft with SPP. Simulations were made to obtain the model speed V and the ship running attitude (H and τ), by giving initially the ship thrust F_T . For the ship in steady state condition, the following equations of motion for forces (x and z directions) and pitch moment for the center of gravity are obtained (see Figure 5.5):

$$\begin{aligned} F_X &= F_T \cos(\tau + \beta) \\ F_Z + F_T \sin(\tau + \beta) + F_B &= W \\ M_G + F_T x L_T + M_B &= 0 \end{aligned} \quad (5.1)$$

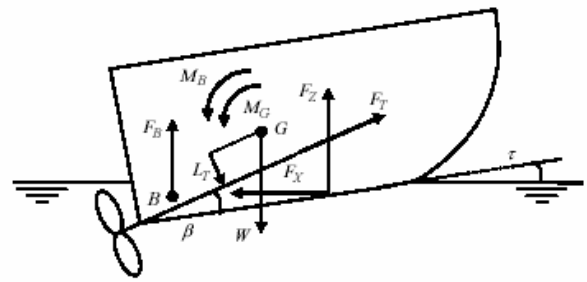


Figure 5.5 Forces and moments acting on running craft (Nozawa and Takayama, 2005).

The computed speed-power curves showed an excellent performance of SPP as compared with the fully submerged propeller for high speed as shown in Figure 5.6.

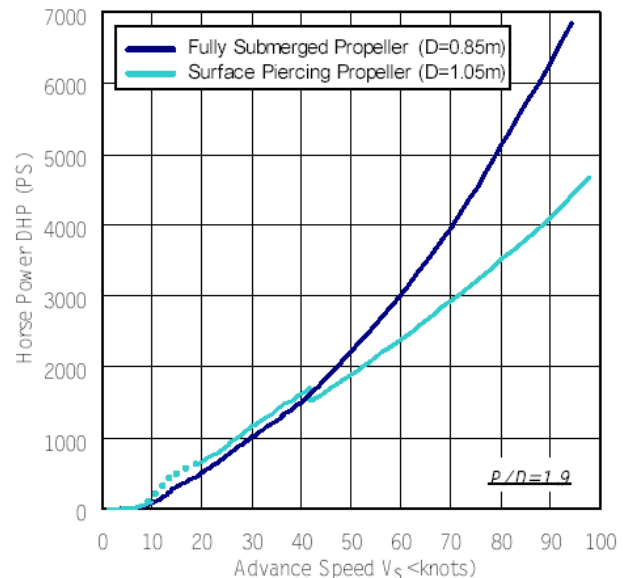


Figure 5.6 Power curve for SPP and fully submerged propeller (Nozawa and Takayama, 2005).

Ferrando, *et al.* (2006) investigated Weber number (W_n) influence on the behavior of SPP based on a series of tests on three models with systematically varying geometries. They found that W_n plays a significant role not only on the position of the critical advance coefficient but also on K_T and K_Q corresponding to fully ventilated regime of SPP.

Ding (2007) presented results of recent research on SPP at the China Ship Scientific Research Center (CSSRC). He presented the de-

velopment of a methodical series of 6-bladed SSPs with varying mean pitch ratios (P/D); 1.1, 1.25, 1.4, 1.55, 1.70 and 1.85. Open water tests were conducted in the CSSRC depressurized towing tank where they can simulate both free surface and cavitation number effects on performance. He tested the 6-bladed SSPs by varying the tip submergence ratio from 0.3 and 0.7 and the shaft inclination angle 0 to 9 deg. By using these charts, new design SPP can be easily made.

He also investigated the effects of Froude number, defined by $F_n = V/(gD)^{1/2}$ where D is the propeller diameter, on propeller open water performance. The F_n was varied from 3.46 to 4.24 with a fixed cavitation number. As shown in Figure 5.7, the K_T , K_Q and η are almost invariant for these F_n range.

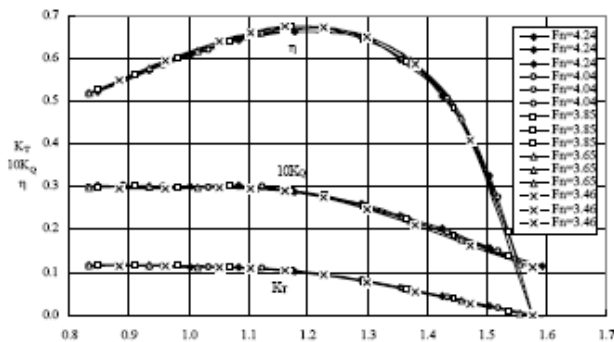


Figure 5.7 Open water performance for different Froude numbers (Ding, 2007).

Ding (2007) also investigated the effects of cavitation number, $\sigma = (p - p_v)/(0.5\rho V^2)$, with a fixed F_n . He tested 4 different σ values, including the atmospheric pressure condition. As shown in Figure 5.8, the effects of σ are also negligible for a given F_n . The author, therefore, concluded that the SSP open water test can be done at atmospheric pressure and that the results will be insensitive to F_n and σ when F_n is greater than ~ 3.5 .

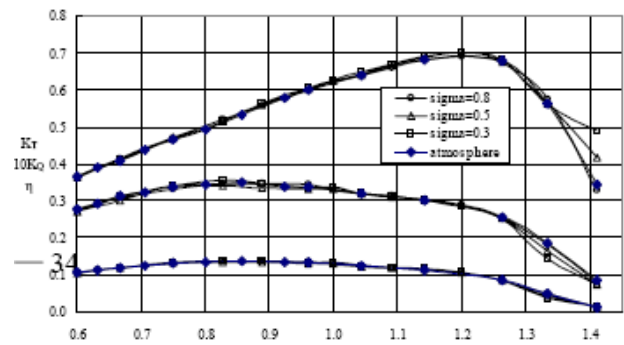


Figure 5.8 Open water performance for different cavitation numbers(Ding, 2007).

Himei, *et al.* (2006) presented a practical SCP design method based on a systematic series designed by their existing method. The authors combined the Trans-Cavitating propeller design concept and NACA-like sections at the blade root to increase the lift-drag ratio. Test results for the new design SCP showed a 1.7% efficiency increase at the design point compared to the SCP designed by the previous method.

5.4 Composite Propellers

There is an increasing interest in using composite materials for marine applications including ship hulls and propellers (Mouritz, *et al.*, 2001). In addition to the advantage of high strength and stiffness, the ability to tailor the propeller/pump blades to deflect in response to load variations in a non-uniform inflow is also attractive. Several papers on composite propellers have recently been published and are reviewed in this section.

Büchler and Erdman (2006) presented various composite propellers and pumps developed over the past 15 years in Germany. Three different kinds of composite propellers were presented; propellers designed for passively adjusting pitch near the tip, surface-piercing controllable pitch propellers, and the rim-driven, hubless propellers (see Figure 5.9). The passive pitch-adapting propellers showed improved low-speed maneuvering. The hubless propellers eliminated the conventional tip-gap cavitation since the blades are attached to the outer

ring. Although there is no hub, the blade tips are concentrated at the centre of the propeller that would potentially cause cavitation. Despite the lack of design and experimental details, the paper indicates that such composite propellers can be designed and fabricated. The authors point out that more research is required in the design and materials. One of the major issues with composite propellers is the cavitation erosion tendency that is much worse than metallic propellers, thus requiring proper protective coatings. The authors indicated that their propellers are coated with polyurethane coating materials. Details of the coating material were not given.



Figure 5.9 Rim-driven hubless composite propeller (inline propeller) (Büchler and Erdman, 2006).

Stauble (2007) presented recent efforts in the German Navy to develop and test full-scale submarine composite propellers. Two 206A Class submarines were installed with composite propellers. The U19 boat installed the first composite propeller in 2002 with the same geometry as a metallic propeller with 100% carbon fibre (see Figure 5.10, left). The composite propeller has been in operation for more than 2 years and ~20,000 nm without any damage or malfunction. More recently in May 2005, the U26 installed a highly damped composite propeller using aramid fiber (Kevlar). Acoustic trials “exceeded all expectation.” In January 2006, a new composite propeller program was initiated to design and install a much larger (~13ft diameter) composite propeller on a 212A Class submarine (see Figure 5.10, right) for a stringent acoustic evaluation. First sea trials were made in August 2006, and first acoustic indications showed a significant improvement. HDW plans to reach a series pro-

duction readiness of the highly damped propeller.



Figure 5.10 Composite propellers installed on German 209A Class (left) and 212A Class (right) submarines (Stauble, 2007).

Chen, Y.H. *et al.* (2006) presented experimental results of pitch-adapting composite propellers. Two model composite propellers, rigid and pitch-adapting, were tested in the NSWCCD 36-inch water tunnel. The test results showed that the pitch-adapting propeller produced better efficiency and cavitation performance than the rigid propeller.

Young (2006, 2007) and Young, *et al.* (2006) developed a coupling algorithm of a BEM and FEM to analyze fluid-structure interaction of cavitating flexible composite propellers in a spatially-varying inflow. BEM was used to solve the fluid problem by decomposing the total velocity into rigid and elastic blade motion. FEM was used to compute the structural deformation of blades and provides new blade geometry for the BEM solver. Iterations were carried out until the solution is converged. The method is able to calculate the hydrodynamic blade loads, stress distributions and deflection patterns. The performance of the two composite propellers designed by Chen, Y.H. *et al.* (2006) was computed in the open water condition and behind a simulated four-cycle wake screen. The predicted blade loads, deflections, cavitation patterns and fundamental frequency in water agreed well with experiments and observations for the case of open water flow. The predicted transient propeller performance be-

hind the wake was in reasonable agreement with experiments. Calculations showed that composite propellers can be properly designed to reduce the sensitivity to inflow and operating conditions. The authors suggested that more systematic validation studies are needed.

5.5 Other Unconventional Propulsors

Some examples of physical-mechanical designs evolved in fish were reported in literature for propulsion and manoeuvring of underwater vehicles.

Highly efficient swimming mechanisms of some pelagic fish can potentially provide inspiration for a design of propulsors that are highly efficient and quiet with a less conspicuous wake. Sfakiotakis, *et al.* (1999) presented an overview of fish swimming and analytical methods that have been applied to some of their propulsive mechanisms.

Mittal, *et al.* (2006) presented preliminary results of their ongoing research program to understand the hydrodynamic performance of the pectoral fin of the bluegill sunfish through a combined experimental-numerical approach and develop a biomimetic robotic fin for use in Autonomous Underwater Vehicle (AUV) propulsion and maneuvering. They measured the motion of the sunfish pectoral fin during both propulsion and maneuvering using two high-speed video cameras recording simultaneously at 250 and 500 fps with 1024 x 1024 pixel resolution. For numerical simulation of the fin motion, they used LES with the immersed boundary method. The key feature of this computational method is that simulations with complex boundaries can be carried out on stationary non-body conformal Cartesian grids and this eliminates the need for complicated remeshing algorithms that are usually employed with conventional Lagrangian body-conformal methods. LES computations of the 3-D wake structure of pectoral fin in steady swimming were in reasonable agreement with experiments.

Zhang, *et al.* (2006) computed unsteady hydrodynamic characteristics of 2-D rigid and flexible flapping foils the Carangiform swimming mode using a RANS solver with SST $k-\omega$ turbulence model. Calculations showed that the rigid foil can produce larger thrust, while the flexible foil can get higher efficiency in certain circumstances.

6. REVIEW PROPULSION ISSUES IN SHALLOW WATER AND FORMULATE RECOMMENDATIONS FOR RESEARCH

6.1 Introduction

Following on from the work of the 24th ITTC Propulsion Committee which addressed propulsion effects of shallow water, there has again been relatively limited published activity

6.2 Influence of Depth on Propulsor Performance

The primary influence of hull-seabed clearance at a given Froude number (F_n) will be the effective change in wake at the propulsor plane. This is influenced by the proximity of the hull to the seabed which influences the development of the upstream hull boundary layer. For larger F_n and with the bow trimmed down separation can occur with significant consequences for propulsor performance. Such effects will only occur at large F_n or very small values of hull-seabed clearance. Such effects are also relevant to waterjet inlets where the upstream influence on the flow of the inlet velocity ratio is paramount.

The wave field generated by the hull will have a significant influence on the wake field as the Froude number based on depth approaches one. For planing and semi-displacement hulls significant changes in trim

can occur with the interaction between propulsor and hull suction.

The interaction of the propulsor with the hull controls the thrust deduction. Such flow interactions are complex and are controlled by the operating condition of the propeller, shaft inclination, hull stern configuration and speed.

6.3 Self-Propulsion Testing in Shallow Water

As part of a programme to investigate wave generation, Chalkias and Grigoropoulos (2007) proposed the use of manned model scale testing in a real sea environment. By a suitable selection of site it is then possible to investigate the influence of water depth. In this initial work propulsion tests were not conducted, however, it is suggested that real-time instrumentation systems are now sufficiently accurate that such tests may offer an interesting avenue for low-cost shallow water testing.

One area of particular interest is the behaviour of planing craft propulsion systems in shallow water. Friedhoff, *et al.* (2007) examined the response of a sports fishing boat in a towing tank in order to better understand hull-propeller interaction and scale effects. The influence of shallow water effects on the transition from displacement to planing and the effect of propeller inclination in self-propulsion tests was of particular interest. The majority of previous work in this area has been carried out at full scale as systematic tests at model scale require depressurised towing tanks to capture cavitation. This work looked at how such tests can be carried out in a standard towing tank as the hydrodynamics are more complex than for displacement ships and the design methodology has to be conservative which for weight sensitive designs reduces operational efficiency. The extensive tests were carried out in the Duisburg tank (190m x 9.8m x 0-1.25m) at speeds up to 15m/s. A lightweight model (2.5m long weighing 20kg) is required to allow for the dynamometer and electric motor. The high speed

carriage allowed accelerations of up to 10m/s^2 which offers enough time to test 2 or 3 propeller rates per run. In order to match the propeller to the full-scale performance specially manufactured propellers were used. An electric motor drive was used for each propeller which required up to 3kW and connection to a different phase supply. The authors based full scale extrapolation on the relevant ITTC procedures. To aid the evaluation of propulsion effects open water tests were done with an axial inflow and with a 10° inclination (see Figure 6.1). Thrust and torque are increased with efficiency little affected. However, beyond the propeller design point (maximum efficiency) the efficiency is higher in the inclined condition.

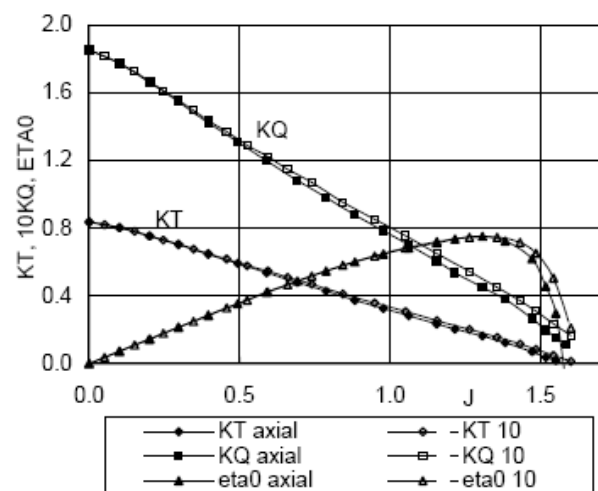


Figure 6.1 Open water diagram in axial and oblique inflow (Friedhoff, *et al.*, 2007).

The trim of the vessel is also influenced by the presence of the propulsor due to hull suction (see Figure 6.2) with a slightly higher trim (bow up) for the propulsion test. Overall, it was found that the transition to the planing regime can be defined for a supercritical speed at which the dynamic trim reaches a maximum. Beyond this speed the delivered power at the propeller is independent of water depth.

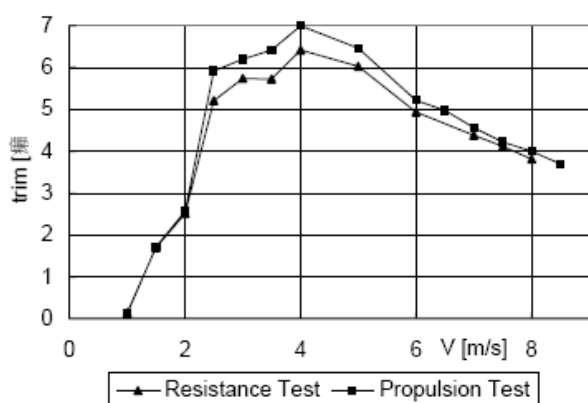


Figure 6.2 Influence of propulsion on running trim (Friedhoff, *et al.*, 2007).

6.4 Low Speed Manoeuvring

An important area of manoeuvring performance is associated with behaviour of ships in the shallow water approaching the ports where the ship is sufficiently close to the seabed that there is significant interaction with the muddy bottom. Delefortrie (2007), Delefortrie and Vantorre (2007) examined the self-propelled performance of a series of three ships: 1/75th scale 6000 TEU container ship, and a tanker form as well as a 1/80th scale 8000 TEU container ship. These tests used a range of under keel clearances (10-32% of draught) above the solid bottom. A variety of combinations of mud layer thicknesses and mud compositions were used. For the range of mud depths hull clearances to the top of the mud layer were in the range of -12% to 21%. Model test speeds were chosen to give two values below the critical wave speed for the mud-water interface and two above. Limited tests were carried out in the slow astern condition. The aim of the research was to develop a suitable model for use with manoeuvring simulation in port approaches. A planar motion mechanism was used to generate the necessary ship motions and tests included bollard pull for a full range of rudder deflections at forward/ahead at 70% and 100% of maximum rpm, stationary tests and harmonic yaw tests. Multi-modal tests were carried out that included harmonic variations of propeller

rate, rudder deflection and longitudinal velocity as well as combinations of all three.

The tests used a 44m long section of the Flanders Hydraulic research shallow water tank with the remaining length divided to store the artificial mud and previously contaminated water. The artificial mud layer was made from a mixture of chlorinated paraffins and petroleum which allowed a wide range of viscosities and densities to be used. All three models tested used a single propeller. It was found that use of the thrust and torque identities gave different answers and so both are used in the thrust and torque models within the mathematical simulation.

It was found that the thrust wake fraction increases with decreasing mud density and small wake fractions when the hull is penetrating the mud. The increase in wake fraction in low density mud was ascribed to the undulations of the mud altering the propeller inflow whereas the high density mud in contact with the propeller giving a greater thrust due to the increase in fluid density passing through the propeller. For the torque wake fraction when penetrating thick mud layers the value approaches one and that the torque increases significantly and this is almost independent of the propeller operating condition.

6.5 Seabed Scour

In the majority of cases slow speed manoeuvring of ships occurs in shallow water. The large energy of the propulsor race has the capacity to scour the local seabed. For example, Hamill, *et al.* (1999) carried out an experimental investigation and developed empirical equations for the prediction of the maximum depth of scour, for any given exposure period, for both free expanding jets and those in close proximity to quays.

Another important influence of knowledge of the propulsive system is in the impact of the resultant wash on the local environment and



scour in particular. Atlar, *et al.* (2007) used LDV to measure the propulsor race at various stations downstream. The tests took place within the Newcastle University cavitation tunnel and simulated a pod arrangement in the wake of a RORO vessel as part of the EU FP5 Optipod project. Such detailed measurements could be made to investigate the influence of water depth for slow speed manoeuvring on the likely scour regime and would complement previous work such as that by Hamill, *et al.* (1999).

Gorski, *et al.* (2005) carried out a detailed investigation comparing propeller performance in bollard conditions in deep and shallow water. These results were compared to theoretical predictions for specified width and depth cross-sections to predict propeller-hull interaction as well as pressure distribution on the waterway bottom and ship sinkage. A combination of potential-based analysis tools are used to account for the presence of the hull, sidewalls and bottom as well as the ship hull. An interactive approach allows the influence of both propeller and a duct to be taken into account. The analysis and experiments were based on a scaled model (1:4.72) of a 20.5 m pushboat of moulded draught 0.6m and breadth 9.0m. The boat uses a central propeller of full-scale diameter 1.1m and two ducted side propellers of full-scale diameter 0.69m. Calculations were carried out for a pushboat and two barges each of $L=48.75\text{m}$, $B=9\text{m}$ and $d=1.4\text{m}$. Propeller calculations used a vortex lattice method and extrapolated bollard pull results from results at three low J conditions. Reasonable comparisons were obtained and the subsequent calculations compared the effect of two ahead speeds, 1.5 and 3.0 m/s for water depths, 1.7, 2.0, 3.6m and canal widths of 9, 20 and 30m. The results indicate that water depth has little influence at bollard pull; the effect of canal banks and bottom on propeller performance is seen at depths below 3.6m and width less than 20m. The propeller thrust at the lowest depth and width is between 17 and 25% higher but efficiency decreases significantly.

6.6 Recommendations for Research

As has been described in Section 2, the improvement in the capabilities of CFD and detailed flow field measurement techniques based on LDV or PIV have significantly improved the ability to quantify the flow regime at the propulsor in shallow water. However, such testing techniques are expensive and for the design of smaller craft cannot be justified. There is considerable scope to develop techniques for concept design that capture the expected flow regime. In the case of craft that operate exclusively in the shallow water regime there is a need to be able to concurrently optimise hull shape and propulsor design.

7. REVIEW THE METHODS FOR PREDICTING THE PERFORMANCE OF SECONDARY THRUSTERS AND COMPARE WITH OPERATIONAL EXPERIENCE

7.1 Introduction

Secondary thrusters were defined by the 24th ITTC Propulsion Committee as devices which produce thrust in any horizontal direction to balance the environmental forces on a ship or an offshore structure for the purpose of station keeping and/or enhanced manoeuvring.

7.2 Thruster Performance

As described by Brix (1993) a thruster, be it as a tunnel within the confines of a hull or mounted on a strut or pod will produce an amount of thrust that is dependent on the relative inflow angle and J . The interesting question is how a thruster is sized to give a specific ship manoeuvring capability. A thruster is required to generate the specified thrust T for a given power which arises from that generated by the rotating propulsor and the remainder from a pressure differential between opposing sides of the hull. The difficulty in practice is in

measuring the net thrust, when installed, and whether it actually delivers what is expected as regards performance. Secondary thrusters on conventional ships are only required for short periods of time whereas dynamic positioning systems for offshore vessels have a much higher duty cycle and overall efficiency is more important.

There is limited data on published thruster performance, although a number of more recent studies are reported later.

Commercial developments of secondary thrusters are concentrating on practical installation issues as well as reducing noise levels and enhancing manoeuvring forces. Installed power levels range up to 3.7MW with diameters to 3.3m with applications as secondary thrusters to use for dynamic positioning, DP. Thrusters can have controllable pitch (CP) or fixed pitch propellers with the CP used for thrusters that experience large service time, for example, with DP. The noise issues are important on passenger craft where cabins maybe located close to thruster tunnels. Such devices require more careful selection of blade sections and knowledge of the flow regime within the tunnel. One solution is to reduce thrust loading by selecting a larger diameter or select a lower tip speed. This may also be a use for electric rim driven thrusters where tip vortex effects are eliminated, Hughes, *et al.*, (2003). Such devices remove the need for asymmetric drive support within the tunnel and improve flow quality as well as freeing up space as the drive is an integral component of the thruster tunnel. Noise is reduced through use of special mounts for the thruster assembly.

7.3 Control of Thruster Systems

A significant amount of published work is focused on methods of representing thrusters as part of control systems. In particular, this is with respect to their application to underwater vehicles. Although the work was applied to the effects of tunnel thrusters for lateral control of

an AUV, Palmer, *et al.* (2008), investigated the transition from ahead control using rear control surfaces to transverse motion using a fore and aft tunnel thrusters. They showed that transition was most effectively achieved using a mixed-mode with transition occurring at as low a forward speed as possible if energy use is to be minimised. This paper provides a useful review of literature used for modelling of thruster performance within control simulations.

It is important for autonomous underwater vehicles to be able to predict thrusters performance as part of the attitude control system. Kim and Chung (2006) propose a predictive model based on only measurable parameters.

7.4 Measurement and Computation of Thrusters

In considering the detailed performance of secondary thrusters it is important to understand the interaction between stators and the drive rotor. These stators are usually used to provide support for the drive shaft or in the case of rim-driven thrusters (Abu Sharkh, *et al.*, 2003) to take the thrust load. As a bi-directional device this provides little scope for enhancing thrust performance but rather is designed to minimise losses. Park, *et al.* (2005) examined, using a 3D incompressible RANS solver, rotor-stator interaction in a ducted marine propulsor. This used a sliding multi-block technique and was validated using time averaged experimental pressure measurements. Figure 7.1 shows the mesh strategy adopted with the sliding zone applied just forward of the rotor leading edge. Figure 7.2 details the complete geometry tested. The authors used a turbine flow to validate their approach as there was no suitable published ducted propulsor experimental or numerical data. Figure 7.3, as part of a mesh sensitivity study, shows the spanwise variation in sectional thrust and torque giving an almost linear drop in performance outboard of $r/R=0.75$. It was noted that the propeller race pressure recovers to the free-stream value at about 4.5D downstream.

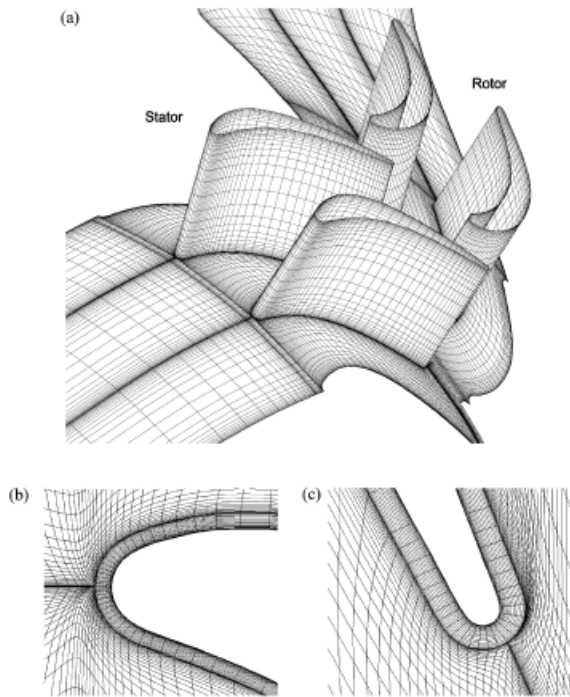


Figure 7.1 Rotor-stator grid system of a turbine. (a) Grid system, (b) leading edge of stator, (c) trailing edge of stator (Park, *et al.*, 2005).

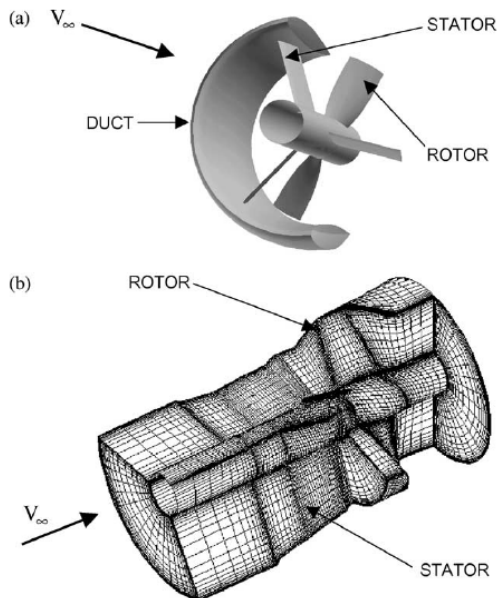


Figure 7.2 Configuration and grid of ducted marine propulsor. (a) Configuration, (b) grid system (Park, *et al.*, 2005).

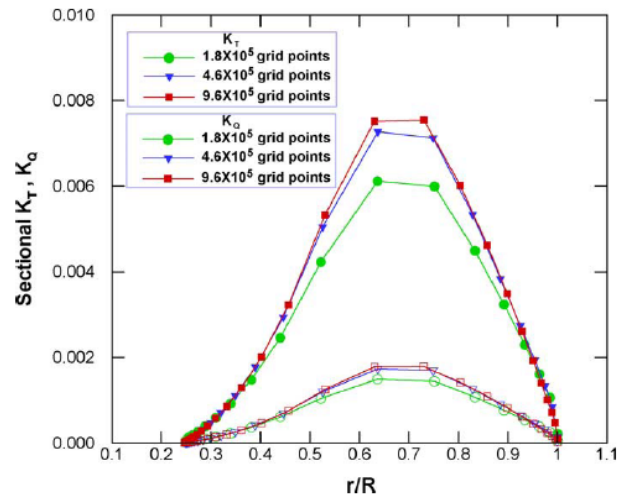


Figure 7.3 Sectional thrust and torque coefficient on the three grid systems (Park, *et al.*, 2005).

In conventional shaft driven thrusters the ability to predict the tip flow effects is crucial. Oweis, *et al.* (2006a) examined the effect of Reynolds number on ducted propulsor tip flow regimes experimentally. A three-bladed ducted rotor was examined in a uniform inflow using a three component LDV over a Reynolds number range of $0.7-9.2 \times 10^6$. The photograph given in Figure 7.4 highlights some of the key flow regimes through use of a lower cavitation number flow. Of particular interest was that there was only a weak influence of Reynolds number on the number and location of tip vortices but that there was an influence on the duct boundary layer. It was found that there was significant unsteadiness in the flow associated with instabilities associated with multiple vortex-vortex interactions. Oweis, *et al.* (2006b) went on to show that without the duct the primary tip vortex increased in strength but for the particular rotor studied the radius of the vortex core does not vary significantly. It is to be expected that the adequate capture by CFD of such complex tip vortex effects will require mesh adaptive techniques as described by Turnock, *et al.* (2006).

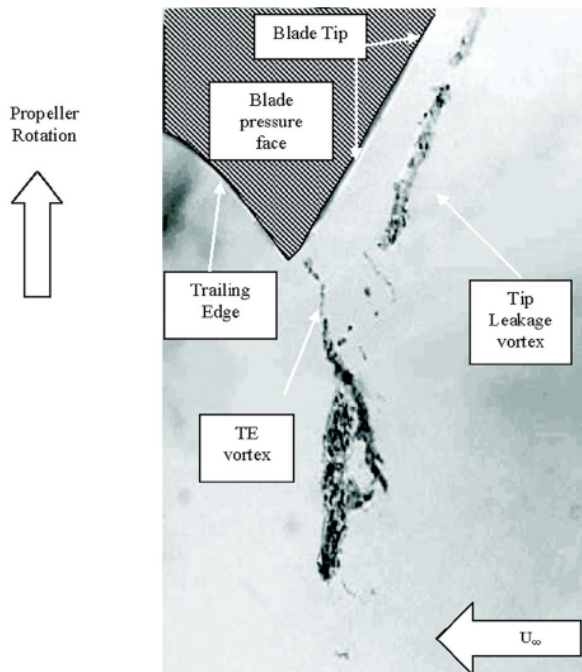


Figure 7.4 A photograph of the blade trailing edge taken through a clear section of the duct ($\sigma = 5.6$) (Oweis, *et al.* 2006a).

Lababidy, *et al.* (2006) also investigated the effect of a duct although on a dynamic positioning thruster. These experimental tests in the IOT towing tank in St John's, Newfoundland and the large cavitation tunnel at INSEAN, Italy examined the effect of advance coefficient and used a stereo PIV system to examine the wake. Figure 7.5 shows the influence on the duct – enhancing efficiency at low J and causing a rapid decrease above $J=0.6$. Reynolds number is shown to have more of an influence in the presence of the duct. In the wake the maximum axial velocity is at $0.6 r/R$ for the open rotor and moves outboard in range $0.6-0.8$ with the duct. The shape of the outboard velocity is similar to that found by Park, *et al* (2005). Figure 7.6 compares the axial wake field at $X/D=0.3$ for three advance ratios. It is interesting to note the effectively stalled rotor with the duct at the highest J .

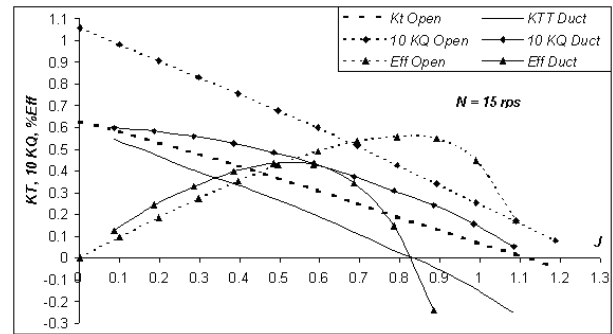


Figure 7.5 DP thruster performance curves with and without a nozzle at $N=20$ rps and $P/D = 1.2$ (Lababidy, *et al.*, 2006).

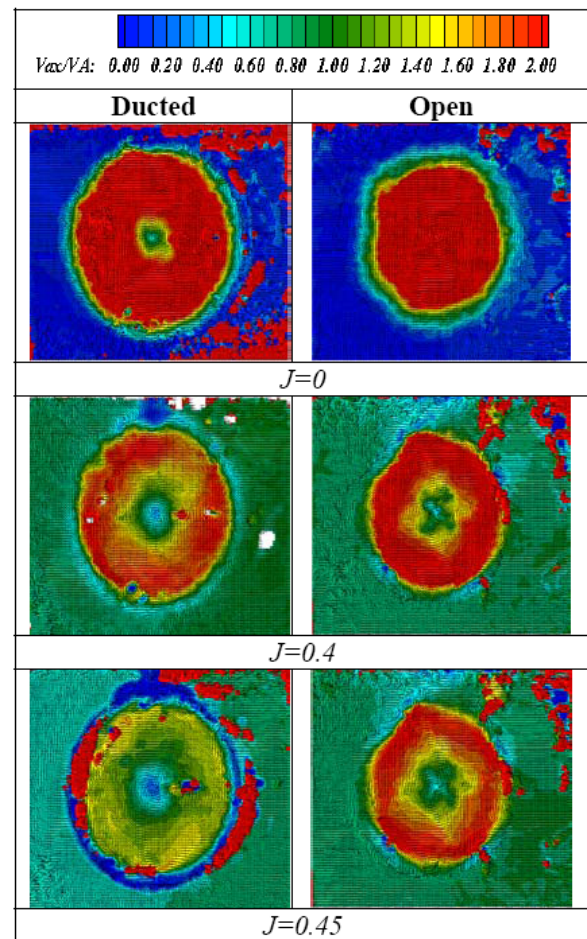


Figure 7.6 Circumferential variation of velocity components around the DP thruster at $X/D = 0.3$ (Lababidy, *et al.*, 2006).

7.5 Bow Thrusters

Thomas and Schmode (2005) examined using a RANS solver the behaviour of a bow thruster through use of a triangular ship section

of 13.18m depth, 12.58m breadth with a 0.51m diameter thruster of length 2.93m. Three different entrance/exit shapes were used (conical, sharp and round). A body force model was used to represent the centrally mounted thruster with values between 1-30kN. This model correctly ranked the entrance shapes from rounded through to sharp with most losses occurring with a sharp edge entrance and hence lowest speed within duct. It also showed that the overall cross force was largest for the conical entrance. The evaluation of the flow homogeneity at the propulsor location would allow matching of the propulsor design to a given duct/hull geometry.

Muller and Abdel-Maksoud (2007) carried out a detailed numerical investigation, using a commercial RANS code, of the flow induced by an integrated thruster. A parametric study was carried out into factors such as the shape of tunnel entrance, tunnel length, inclination of the vessel side and the shape and position of the tunnel protective grids. Figure 7.7 shows a cross-section through the mesh for one configuration. Typical mesh size was 2M cells for the rotating blades and 3.2-4.6M for the remaining stationary domain.

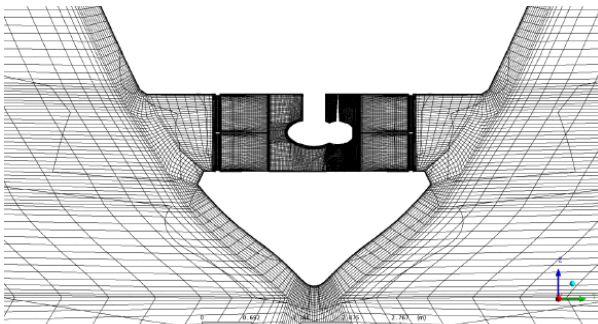
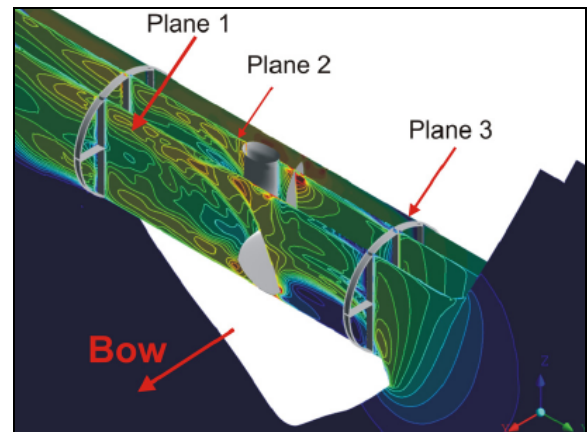


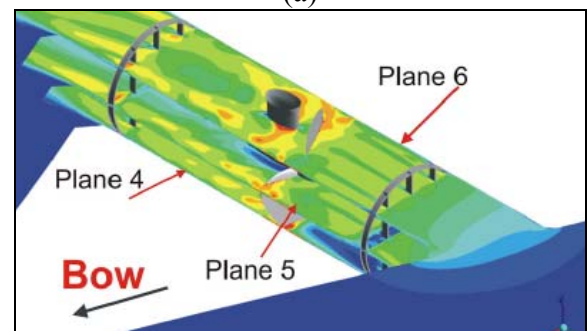
Figure 7.7 Vertical section of the numerical grid of the reference ship (Muller and Abdel-Maksoud, 2007).

Figure 7.8 shows vertical and longitudinal planes that characterise the flow regimes through the tunnel with thrusters working. The study could identify specific flow features –for example flow separation was more likely in a short tunnel. Wall inclination was important as the higher the thrusters were mounted the clos-

er to a vertical side. This results in an increase in thrust force on the hull and less generated on the blades, although this was the dominant component (up to 90%) for all configurations tested. It was found the most effective length of tunnel was between 2.6 and 4.2D. The inlet shape was important with higher residual thrust for conical inlet as opposed to a sharp intersection. The presence of the protective grid also has to be considered as its additional resistance can reduce the effectiveness. Use of the computations allowed guidance to be made as to the most effective position to reduce losses in overall thrust.



(a)



(b)

Figure 7.8 shows the velocity field in a vertical plane (a) and horizontal plane (b) (Muller and Abdel-Maksoud, 2007).

Nielsen (2005) examined the effect of the flow induced by a bow thruster on a vertical quay wall (Figure 7.9). Experimental tests using a 1:25 scale model of the bow region was used. Velocity measurements were made using a calibrated electromagnetic velocity meter.

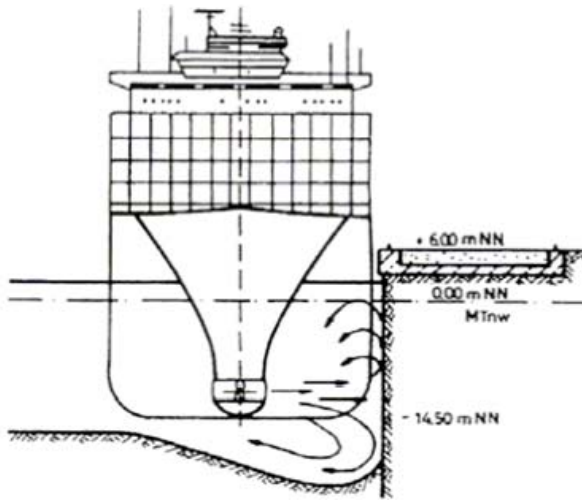


Figure 7.9 The working of a bow thruster at a vertical quay wall (Nielsen, 2005).

7.6 Ventilation of Dynamic Positioning (DP) Thrusters

The effect of forced heave on a ventilating thruster was investigated experimentally by Koushan (2006). A high speed camera was used to visualise the ventilation as the thrusters moved in and out of the water in a sinusoidal manner. The tests used a 0.25m D propeller with P/D of 1.1 and BAR 0.595. It was found that there were significant fluctuations in axial force and that these were due mainly to ventilation rather than the heave motion. The condition at which ventilation initiates leads to the highest fluctuations. Ruth and Smogeli (2006) examined the ventilation of controllable pitch thrusters suitable for dynamic positioning systems. These DP systems in severe weather can experience large changes in propeller loading that the CP control system has to respond to. From their experimental results a ventilation model was developed and scaling discussed. The model predicts the loss in thrust and torque as functions of a diameter-based Froude number and the local axis submergence ratio h/R and was considered suitable for use in developing control laws.

7.7 Recommendations

No published data was found that could aid in comparing operational experience with performance prediction. This would be a useful study that would allow more effective design decisions.

The application of CFD to thrusters analysis appears to be an area for future developments as computational power becomes more affordable. However, it is clear that there is a lack of knowledge as to possible scale effects and it is recommended that research focus on how model scale manoeuvring tests can take due account of the scaled performance of the thrusters. Such inadequacies are important for the design of DP thrusters systems with high duty cycles.

8. FINALISE THE BENCHMARK TESTS FOR WATERJETS AND ANALYSIS OF THE DATA

8.1 Background

The objective of the 24th ITTC Specialist Committee on Validation of Waterjet Test Procedures was to develop and provide proven procedures for the determination of the powering characteristics of waterjet-propelled vessels. To meet this objective, a series of standardization tests were conducted by the following nine ITTC member organizations:

- CEHIPAR – Canal de Experiencias Hidrodinamicas de El Pardo, Spain
- HMRI – Hyundai Maritime Research Institute, Korea
- INSEAN – Italian Ship Model Basin, Italy
- KRISO – Korea Research Institute of Ships and Ocean Engineering (now MOERI), Korea
- KRSI – Krylov Research Shipbuilding Institute, Russia



- MARIN – Maritime Research Institute, the Netherlands
- NSWC – Naval Surface Warfare Center (David Taylor Model Basin), U.S.A.
- SSMB – Samsung Ship Model Basin, Korea
- SVA – Schiffbau–Versuchsanstalt Potsdam GmbH, Germany.

A scale model of the U.S. Navy's research vessel Athena (LOW=46.9m) (Figure 8.1) was used for these tests. An 8.556 scale model (LOW=5.49m) was fitted with a pair of axial-flow waterjets that had a 7 blade impeller and 11 blade stator (Figure 8.2).



Figure 8.1 Full-scale Athena (upper, with conventional propellers) and model scale with waterjets).



Figure 8.2 Waterjet impeller and stator/nozzle

Two Athena ship models, designated Model 1 and Model 2, were constructed and circulated.

Model 1 was shared by the European participants, and Model 2 by the U.S. and Asian participants. Both models were fitted with an identical waterjet system. Two participants (SVA and KRSI), due to schedule slips, were unable to receive the test model in time to have their self-propulsion test results presented in the 24th ITTC Waterjet Committee Report. These results have been added to the database and are presented here completing the standardization effort of the 24th ITTC Waterjet Committee.

The details and all essential technical data concerning all of the tests performed were presented in the 24th ITTC Waterjet Report. Due to the limited data submitted at other speeds, the design speed Froude number of 0.60 became the primary reference speed.

8.2 Summary of the Findings

The self-propulsion experiment was subdivided into six components:

- Bare Hull Resistance Tests
- Bare Hull Inlet Velocity Survey
- Working Inlet Velocity Survey
- Jet Velocity Survey
- Momentum Flux Calculations
- Full Scale Predictions

The major findings for each experimental component are summarized below.

8.2.1 Bare Hull Resistance Tests

The test displacement varied by 30kg (17.1 LT full scale) (Figure 8.3). There was a lack of agreement in how to determine the model test weight to be used at each facility.

The bare hull resistance tests were supposed to be conducted with the inlet and nozzle covered. Some participants, however, conducted the testing with inlet and nozzle open so that the duct was filled with water.

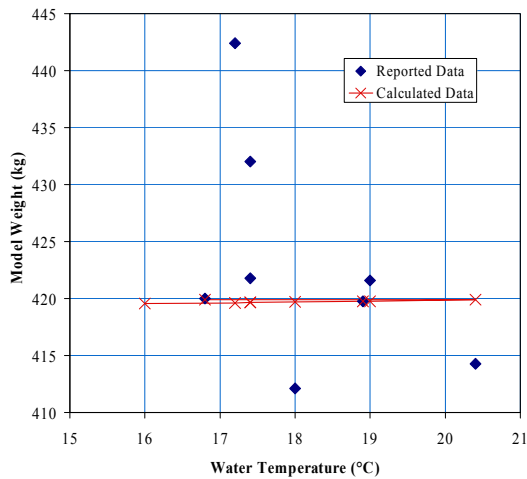


Figure 8.3 Model test displacements.

There are two trend lines for the resistance data. One is approximately 7.0% higher than the other (Figure 8.4). Data from the small basins showed higher drag than that from large basins.

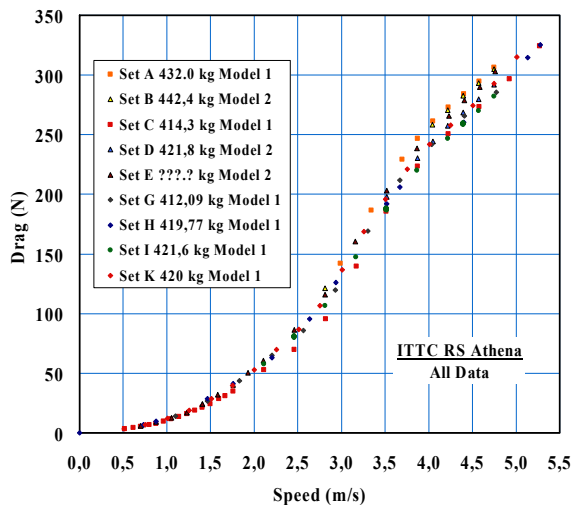


Figure 8.4 Measured bare hull resistance for both Model 1 and Model 2.

There is a 4.5% scatter band in the resistance measurement. The scatter is greatly reduced to 1.0% for the higher group (small basins) and 1.7% for the lower group (large basins). These differences appear to be due to blockage effects (Figures 8.5 and 8.6).

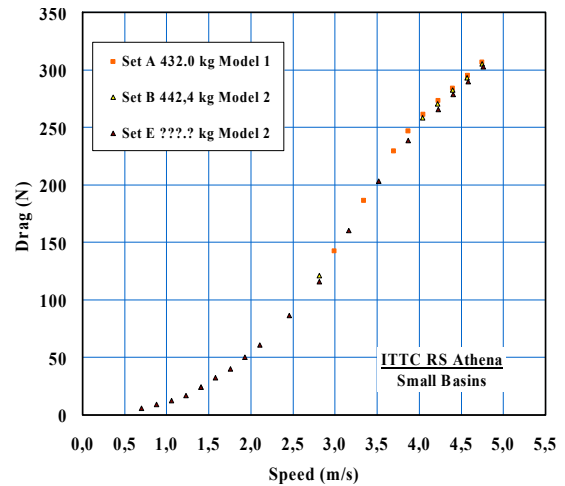


Figure 8.5 Drag from small basins (upper trend line).

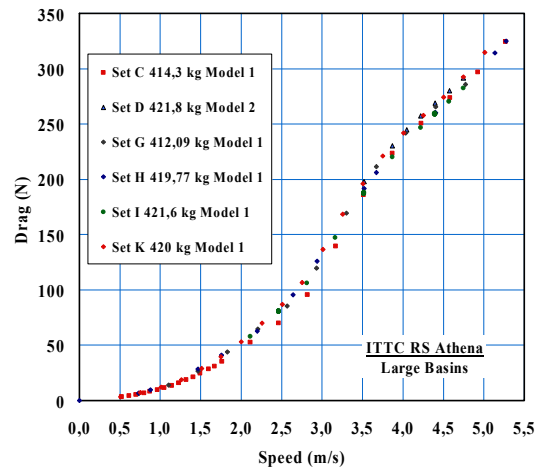


Figure 8.6 Drag from large basins (lower trend line).

There is a considerable scatter in both the trim (pitch) and heave results (Figures 8.7 and 8.8). Running trim has an overall scatter of 10.6% and heave 117%, at a Froude number of 0.60. If the outliers are not accounted for, this is reduced to 2.9% for pitch and 55% for heave.

The scatter appears to be due to the difference in measurement methods. Two methods were used; one is accurate determination of the longitudinal location where the fore and aft displacement was measured (Figures 8.9 and 8.10) and the other is a direct measurement of heave and pitch (Figure 8.11 and 8.12). Direct measurements showed much less scatter than ‘fore and aft’ measurements.

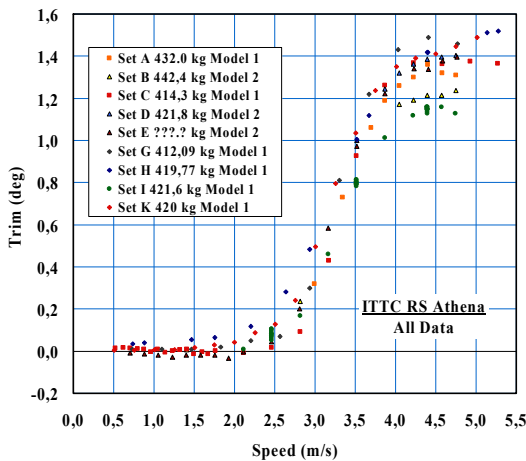


Figure 8.7 Measured trim.

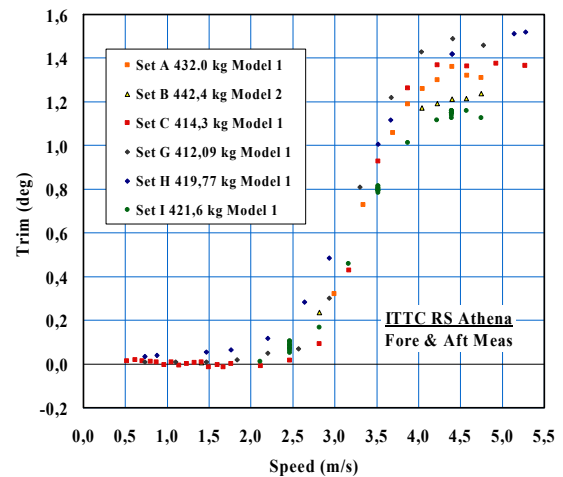


Figure 8.9 Trim by "Fore and Aft Method".

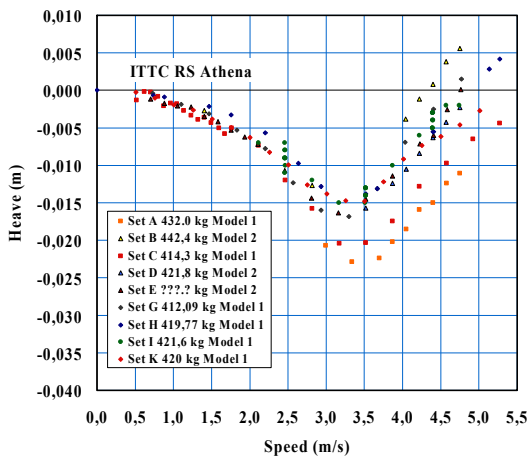


Figure 8.8 Measured heave.

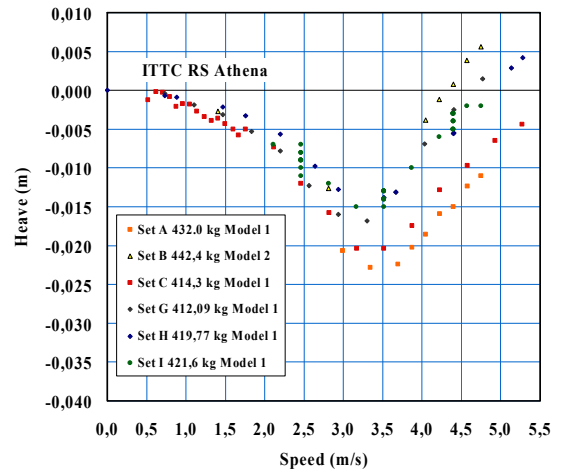


Figure 8.10 Heave by "Fore and Aft Method".

8.2.2 Bare Hull and Working Inlet Velocity Survey

The inlet velocity (boundary layer) profiles with and without waterjet operation are shown in Figures 8.13 and 8.14. The scatter in the inlet velocity profiles for the bare hull (without waterjet operating) is much smaller (Figure 8.13) than that for the 'working inlet velocity' (with waterjet operating) (Figure 8.14). The profile and the height to the free stream appear to be sensitive to transverse location of the working inlet.

The ability to consistently obtain, through different tests, the shape of the velocity profile for the bare hull is very good. Using the bare hull data, the sensitivity of the velocity terms to shape was found to be 0.54% for the average velocity, 0.45% for the momentum velocity, and 0.3% for the energy velocity.

The agreement in the velocity profile shape is not as good in the case of the working inlet as the bare hull case. The sensitivity of the velocity terms to shape was found to be 0.97% for the average velocity, 0.99% for the momentum velocity, and 1.00% for the energy velocity using working inlet data.

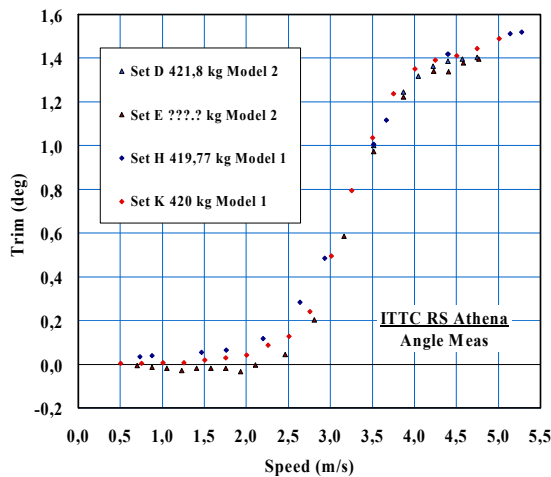


Figure 8.11 Trim by “Direct Method”.

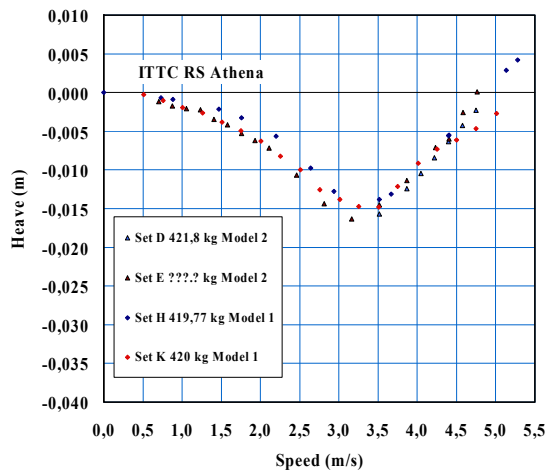


Figure 8.12 Heave by “Direct Method”.

8.2.3 Jet Velocity Survey

The jet velocity surveys in these data sets (Figures 8.15 and 8.16) could not be integrated to estimate the flow rate accurately enough for the momentum flux method due to errors in the measurement of the velocities near the jet boundaries.

It was determined that using the measured bollard thrust to calculate the flow rate along with a multi-port velocity reference probe in the jet to account for changes with forward speed, resulted in the lowest overall uncertainty for the flow rate measurement.

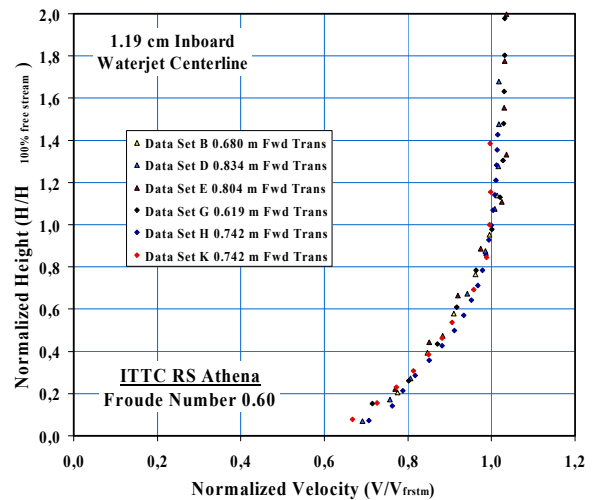


Figure 8.13 Inlet velocity profiles without waterjet operating.

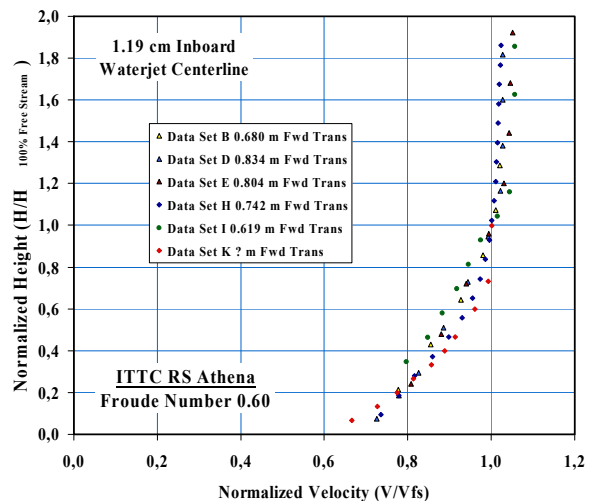


Figure 8.14 Inlet velocity profiles with waterjet operating.

The overall scatter was 3.8% on the normalized axial velocity. The average momentum non-uniformity factor, c_{m7} was 1.004, and the average axial energy non-uniformity factor c_{ex7} was 1.005 and the average total energy non-uniformity factor c_{e7} was 1.01.

8.2.4 Momentum Flux Calculations

The agreement among three different methods for flow rate determination was very good. They are direct measurement of flow, integration of the measured velocity field within the duct, and determination of apparent flow rate from the bollard thrust.

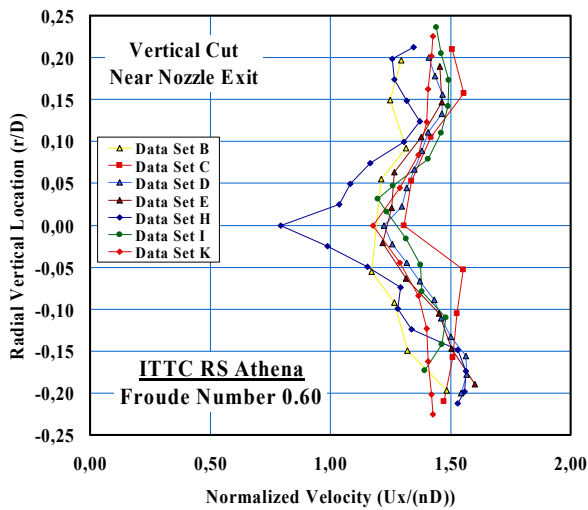


Figure 8.15 Normalized jet velocity profiles – vertical cut.

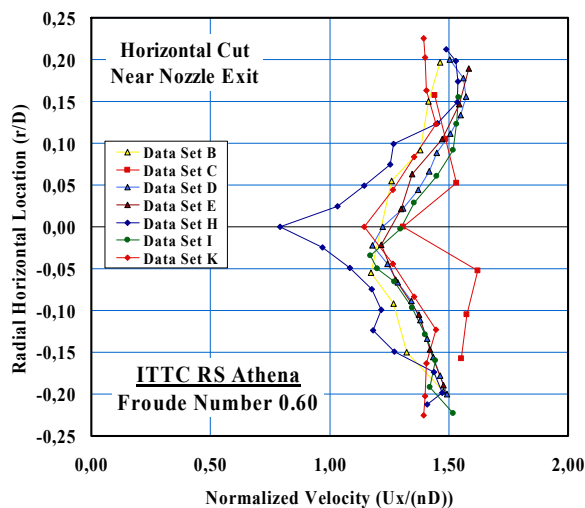


Figure 8.16 Normalized jet velocity profiles – horizontal cut.

There is a 3.5% scatter in the model waterjet speed, and a 4.4% scatter in the volume flow rate for the model at the self-propulsion point for a Froude number of 0.60.

There appear to be numerous problems, not with the execution of the experiments, but with the subsequent analysis which results in a large spread of 44.6%.

There is also a problem with determining the tow force. Although the tow force problem did not adversely affect the determination of flow rate, the impact on the final result of an improper estimate of the flow rate propagates by

the second and third power. The scatter in the estimated model thrust is 18.5%.

It is unclear whether the respondents applied the corrections for the asymmetry of the flow in the inlet and jet flow. There was insufficient information provided to determine this. Considering the fact that those who did expand the data to full scale often used the same IVR and JVR model and full size, however, it is strongly suspected that they did not.

The scatter in IVR at Station 1 was 7.6%. Everyone except one data set had the same reported IVR for model and ship. The scatter in the NVR, since no one really estimated the effect of the *vena contracta*, was 4.7 %.

8.2.5 Full Scale Predictions

Few full-scale performance predictions were submitted. The estimation of full-scale resistance was good. Overall, there was a scatter band of 6.6%. If the two divergent trend lines are separated, however, the scatter reduces to 1.5% and 3.0% for the upper and lower curves, respectively.

The scatter in full-scale flow rate is 4.9%, in full-scale thrust is 16.4%, and in full-scale jet system power is 29.3%.

It appears that the Reynolds number scaling effects from model to ship are not universally accounted for. It also appears that there is a problem in determining the self-propulsion point.

The differences in model self-propulsion point will overshadow any of the scaling effects since it affects the flow rate by 5.5%, whereas Reynolds scaling will account for only 2.2%. Since the thrust varies with approximately flow rate squared and the power with flow rate cubed, it is crucial that the tow force and model self-propulsion point be determined properly for an accurate full-scale power prediction.

8.3 Effect of the New Results

The addition of the two new sets of data did not impact the conclusions presented by the 24th ITTC Specialist Committee on Validation of Waterjet Test Procedures. In fact, the same issues were present in the new sets of data as found in the previous data.

If ship resistance is required, then the old issues that impact all resistance tests are obviously present when it is to be applied to a waterjet-propelled vessel. Issues related to towing tank blockage effects are not unique to the waterjet-driven vessels, but are common for any type of ships.

The accurate measurement of flow rate is essential to waterjet powering performance prediction. In the absence of internal velocity survey, the "Bollard Method" appears to be the best method until a different approach is developed.

The determination of tow force and the self-propulsion point is the single most important problem that needs to be addressed. This is not an experimental issue, but one of analysis.

In the appropriate application of Reynolds number scaling differences when going from model to ship for the waterjet system, as well as factoring in the effects of momentum and energy non-uniformity in the inlet and jet flow are not universally used. This is a problem of educating those carrying out the analysis to ensure a rigorous, physically correct approach is adopted for performance prediction

9. CONCLUSION

There is diverse and wide ranging research within the remit of the Propulsion Committee. The report has identified specific areas where significant advances have been made. These areas include axial-flow waterjets, podded propulsors, advanced blade sections, composite propellers and propeller blade coatings. The generic technologies to support such advances

include new and improved experimental techniques as well as the rapid developments in marine computational fluid dynamics (CFD) where far greater detail and resolution is now possible. The need to understand exactly what level of flow detail is required to resolve a design computationally still needs detailed consideration. In the fullness of time the final proceedings of the SIMMAN 2008 Workshop will provide further evidence to help resolve this. An achievement that can be highlighted is that ship self-propulsion CFD can now be considered a viable design analysis that accounts for hull-propeller-rudder interactions. More validations are required to demonstrate the accuracy of the predictions of these complex interactions. Advanced CFD capabilities should now allow a limited study of scale effects to be made.

Advances in PIV continue with the ability to achieve greater temporal resolution and systems that capture all three velocity components. This allows much greater understanding of tip vortex and cavitation behaviour. Likewise, use of high speed video photography is becoming more accessible and again permits greater physical understanding. Of particular interest was the use of such techniques to study propeller crashback and to provide at least qualitative methods of comparing flow fields to the application of LES to the same problem.

Advances in LES capability enabled the first-ever accurate computations of highly unsteady separated flow around an open propeller in crashback operation. Further improvements are required to model the entire hull and propellers in crashback mode.

The propeller terminology and nomenclature have been thoroughly reviewed and differences with ISO were explicitly captured. It is concluded that the ISO procedure provides insufficient clarity with regard to detailed aspects of section shape. A method of describing the blade geometry in non-cylindrical sections has been identified for propellers with highly tapered hub such as podded or ducted propulsors.



In reviewing the Propulsion Test Procedure some potential issues were identified associated with bollard pull testing and full-scale bollard predictions. It was recommended that the self-propulsion test procedure be further extended to include the bollard pull tests with conventional open/ducted propellers and/or azimuthing podded thrusters and CRP systems.

The current Propeller Open Water Test Procedure has been reviewed and found that the current procedure is valid only for towing tank applications. Open water tests can also be carried out in the cavitation tunnel if a suitable towing tank facility is not available. Therefore the procedure was extended to cavitation tunnel applications with proper account taken of the blockage (wall) effects.

Although no changes were proposed to the LDV Guide itself the Committee reviewed major advances in LDV and PIV measurements of propeller and fully-appended hull flow.

The review of the High Speed Marine Vehicles Propulsion Test (7.5-02-05-02) was challenging because of insufficient information in the existing document. In this case mostly clarifications were made with no significant changes to actual procedure. However, it should be recognised that a number of aspects of this procedure would benefit from more detailed research especially on the effect of shaft inclination on actual effective wake analysis.

The Committee identified archival-quality experimental data that can be added to the ITTC benchmark data for CFD validations. They are (1) KRISO containership, KCS, self-propulsion test data presented to the CFD Workshop Tokyo 2005 (Hino, Ed., 2005), (2) the multi-partner collaborative ship maneuvering test data presented to the SIMMAN 2008 Workshop and further reported on in the 25th ITTC Manoeuvring Committee report, (3) hull-propeller-rudder interaction test data on MO-ERI 138K LNG Carrier (KLNG) (Kim, *et al.*, 2007), and (4) PIV data for unsteady flow around open propeller (Jessup, *et al.*, 2004) and

ducted propeller at crashback conditions (Jessup, *et al.*, 2006).

An experimental study of propeller coating with new environmentally friendly antifouling paint type showed some promise but particular care had to be taken with the trailing edge treatment to avoid singing. When applied correctly propeller performance was maintained. In order to quantify the effect of such coatings at model scale one should simulate the surface roughness corresponding to in-service propellers.

Computational methods to predict flow characteristics around ships are increasingly used today. In this respect, results of the CFD Workshop Tokyo 2005 showed that methods predict well self propulsion factors of a containership without effect of a rudder compared to the experimental results. However some differences are found in relative rotative efficiency values. Rudder effects were also studied in other studies. It can be concluded that rudder effect on the propulsive performance of a ship cannot be ignored and is an important parameter for better prediction.

Some improvements were reported in the numerical modeling in the area of bubble-propeller interactions. Computations were used to show that bubbly flow causes a degradation of propeller performance, and that the propeller action changes the bubble size distribution and increases the void fraction downstream of the propeller compared to that upstream. One of the important parameters for propeller numerical studies is modelling of turbulence. Investigations indicate that discrepancy between calculated and measured values of propeller performance parameters depends on the choice of turbulence model.

The experimental work on secondary thrusters looking at low speed manoeuvring and including such effects as muddy bottoms coupled with the demonstrated capability to use CFD to model complete hull-thruster tunnel—stator-grill-rotor systems indicate that no specific task

should be assigned in this area. Potential improvements in efficiency can be identified through the possible application of rim driven rotors.

The consideration of shallow water has shown that if the appropriate wake field including vessel sinkage and trim are accounted for then propulsive effects can be considered in a standard manner. However, for very shallow model scale behaviour of the interaction between model scale hull boundary layer and seabed needs careful consideration (see work on muddy bottoms). It is possible that hull flow separation occurs that will influence propulsive performance. Only a limited number of commercial testing facilities worldwide regularly carry out work using shallow water tests with much of this work focused on inland waterway manoeuvring.

The remaining work of the waterjet benchmark case has been completed and missing data incorporated. The addition of the two new sets of data did not impact significantly on the conclusions presented by the 24th Specialist Committee on Validation of Waterjet Test Procedures.

It was evident from the review of the guidelines for the use of LDV that techniques have moved on and that these should be expanded to include other uses of coherent optical light as well as digital photography. This could be best addressed by a specialist group bringing together the worldwide expertise in the use of Laser/Optical systems for flow measurements for maritime applications in towing tank, circulating channels, cavitation and wind tunnels. Due reference should be made to the published literature on the physics of such systems.

In looking to future areas for investigation the Committee would identify the following aspects as likely to be of interest.

An area to examine is the application of additional propulsive devices such as kites both for retrofitting and new build. This changes propeller design –what is optimum operating

condition when kite device may or may not be assisting propulsion.

The likely expansion in use of composite propellers (reduced weight/cost savings) requires a reappraisal of model test techniques with greater understanding of fluid-structure interaction of composite propeller blades for both dynamic (hydroelastic response) and the mean loaded shape. This is important as larger diameter propellers are considered for production. Future research should include accurate modeling of fluid-structure interactions, hydrodynamic design and performance prediction capability including the displacement of blade tips, scaling of hydrodynamics and structural fabrication, and cavitation erosion and prevention.

An examination should be made of how small changes in overall propulsive efficiency (QPC) can be achieved through synthesis of CFD and model scale techniques. This is in light of significant increase in marine fuel costs and pressure to reduce emissions/impact on climate change of marine trade. In particular how can a much more detailed knowledge of scale effects available through application of CFD to stern arrangement/model propellers be used to best advantage.

There is a lack of suitable studies on appendage propeller hull rudder interaction with respect to scale issues for CFD validation. It is likely that SIMMAN 2008 Workshop will indicate that current CFD mesh size/cost restricts resolution of complete stern arrangements (rudders-shafts-brackets) essential for correct propulsion analysis. There may be scope for a workshop type activity to better understand the detailed modeling of these interactions through use of larger scale model testing.

Further work is still required to translate the waterjet scaling analysis into a robust approach. Specific areas of weakness identified in the benchmarking exercise still need to be addressed. The considerable interest worldwide in autonomous underwater vehicles requires



better methods to assess propulsive efficiency of such systems and in particular how biometric propulsive devices can be assessed.

9.1 Recommendations to the Conference

Adopt the improved definitions 7.5-01-02-01: Terminology and Nomenclature of Propeller Geometry.

Adopt the improved procedure 7.5-02-03-01.1: Propulsion Test.

Adopt the improved procedure 7.5-02-03-02.1: Propeller Open Water Test.

Adopt the improved procedure 7.5-02-05-02: High Speed Marine Vehicles Propulsion Test.

10. REFERENCES

- Abbott, I.H. and von Doenhoff, A.E., 1959, Theory of Wing Sections, Dover Publications, Inc. New York.
- Abdel-Maksoud, M., Hellwig, K. and Blaurock, J., 2004, "Numerical and Experimental Investigation of the Hub Vortex Flow of a Marine Propeller", Proc., 25th Symp. on Naval Hydrodynamics, St. John's, Canada.
- Abu Sharkh, S.M., Turnock, S.R. and Hughes, A.W., 2003, "Design and performance of an electric tip-driven thrusters", Proc., the Institution of Mechanical Engineers, Part M: J. of Engineering for the Maritime Environment, 217, (3), 133-147.
- Atlas, M., Glover, E.J., Candries, M., Mutton, R. and Anderson, C.D., 2002, "The Effect of a Foul Release Coating on Propeller Performance", Proc. of ENSUS, University of Newcastle upon Tyne, UK.
- Atlas, M., Glover, E.J., Mutton, R., and Anderson, C.D., 2003, "Calculation of the Effects of New Generation Coatings on High Speed Propeller Performance", Proc., 2nd Int'l Warship Cathodic Protection Symp. and Equipment Exhibition, Cranfield University, Shrivenham.
- Atlas, M., Mutton, R. and Downie, M., 2005, "Discussion to the 24th ITTC Propulsion Committee", Proc., the 24th ITTC, Vol. III, Edinburgh, UK.
- Atlas, M., Wang, D., and Glover, E.J., 2007, "Experimental investigation into the impact of slipstream wash of a podded propulsor on the marine environment", Proc., Institution of Mechanical Engineers: J. of Engineering for the Maritime Environment, Vol. 221 Part M, 67-79.
- Bensow, R.E., Liefvendahl, M. and Wikström, N., 2006, "Propeller Near Wake Analysis Using LES With a Rotating Mesh", Proc., 26th Symp. on Naval Hydrodynamics, Rome, Italy.
- Black, S., Shen, Y. and Jessup, D., 2006, "Advanced Blade Sections for High Speed Propellers", Proc., Propeller/Shafting 2006 Symp., SNAME.
- Bobanac, N., Sambolek, M., Radic, S. and Beatorovic, I., 2005, "Cost effective full scale observation and recording of propeller blade cavitation", Proc., 12th Int'l Congress of the Int'l Maritime Assoc. of the Mediterranean (IMAM 2005), Lisboa, Portugal.
- Brewton, S., Gowing, S., and Gorski, J., 2006, "Performance Predictions of a Waterjet Rotor and Rotor/Stator Combination Using RANS Calculations", Proc., 26th Symp. on Naval Hydrodynamics, Rome, Italy.
- Brix, J.E. (ed.), 1993, Manoeuvring Technical Manual, Seehafen Verlag.
- Bulten, N. and Verbeek, R., 2007, "Development of new waterjet installations for applications with reduced transom width", Proc., 9th Int'l Conf. on Fast Sea Transportation

- FAST2007, Shanghai, China.
- Büchler, D. and Erdman, L., 2006, "Composite Propeller New Features and Properties - Specific Design and Experiences", Proc., Propeller/Shafting 2006 Symp., SNAME.
- Chalkias, D.S. and Grigoropoulos, G.J., 2007, "Experimental Investigations of the Waves Generated by High-Speed Ferries", Proc., 9th Int'l Conf. on Fast Sea Transportation FAST2007, Shanghai, China.
- Chao, K.Y., 2005, "Numerical Propulsion Simulation for the KCS Container Ship", Proc. of CFD WORKSHOP TOKYO 2005, Tokyo, Japan.
- Chen, Y.H., Neely, S.K., Michael, T. J., Gowing, S., Szwer, R. P., Büchler, D. and Schult, R., 2006, "Design, Fabrication and Testing of Pitch-Adapting (Flexible) Composite Propellers", Proc., Propeller/ Shafting 2006 Symposium, SNAME.
- Chen, C.T., Hwang, J.L., Hsin, C.Y., and Lin, C.C., 2006, "The effect of an unconventional propeller tip geometry on tip flow phenomena", Proc., 3rd Asia-Pacific Workshop on Marine Hydrodynamics, Shanghai, China.
- Cusanelli, D., Carpenter, S. and Powers, A., 2007, "Axial Waterjet (AxWJ) Model 5662 and Mixed-Flow Waterjet (MxWJ) Model 5662-1: Comparisons of Resistance and Model-Scale Powering with Propulsion Nozzle Designs", NSWCCD-50-TR-2007/076.
- Dang, J. and Laheij, H., 2004, "Hydrodynamic Aspects of Steerable Thrusters", Proc., Dynamic Positioning Conf., Houston, USA.
- Delefortrie, G., 2007, "Manoeuvring behaviour of container vessels in muddy navigation areas", PhD Thesis, Ghent University.
- Delefortrie, G. and Vantorre, M., 2007, "Modeling the manoeuvring behaviour of container carriers in shallow water", J. of Ship Research, Vol. 51, No. 4, pp. 287-296.
- Deniset, F., Laurens, J.-M. and Romon, S., 2006, "Ranse-BEM Approach for Analysis of Strut Behaviour of Podded Propulsors", Proc., TPOD - 2nd Int'l Conf. on Technological Advances in Podded Propulsion, L'aber Wrac'h, Brest, France.
- Ding, E., 2007, "A Series of Surface Piercing Propellers and Its Application", Proc., 9th Int'l Conf. on Fast Sea Transportation, FAST 2007, Shanghai, China.
- EC, 2003, "TBT Regulation Consequences-Regulation (EC) No 782/2003 of the European Parliament and of the Council of 14 April 2003 on the Prohibition of Organo-tin Compounds on Ships", European Commission Dir.-General for Energy and Transport.
- Farin, G., 1990, Curves and Surfaces for Computer Aided Geometric Design: A Practical Guide, Academic Press.
- Felli, M., Greco, L., Colombo, C., Salvatore, F., Felice, F. D., and Soave, M., 2006, "Experimental and Theoretical Investigations of Propeller-Rudder Interaction Phenomena", Proc., 26th Symp. on Naval Hydrodynamics, Rome, Italy.
- Ferrando, M., Viviani, M., Crotti, S., Cassella, P. and Caldarella, S., 2006, "Influence of Weber Number on Surface Piercing Propellers Model Tests Scaling", Proc., 7th Int'l. Conf. on Hydrodynamics, Ischia, Italy.
- Flikkema, M.B., Holtrop, J., and van Terwisga, T.J.C., 2006, "A Numerical Model of Tractor Pods for Power Prediction", Proc., TPOD - 2nd Int'l Conf. on Technological Advances in Podded Propulsion, L'aber Wrac'h, Brest, France.
- Friedhoff, B, Henn, R., Jiang, T. and Stuntz, N., 2007, "Investigation of Planing Craft in



- Shallow Water”, Proc., 9th Int’l Conf. on Fast Sea Transportation (FAST 2007), Shanghai, China.
- Frolova, I., Kaprantsev, S., Pustoshny, A. and Veikonheimo, T., 2006, “Development of Propeller Series for Thrusters Azipod Compact”, Proc., TPOD – 2nd Int’l Conf. on Technological Advances in Podded Propulsion, L’aber Wrac’h, Brest, France.
- Fung, S., Karafiath, G., Cusanelli, D. and McCallum, D., 2007, “JHSS (Joint High-Speed Sealift Ship) Hull Form Development, Test and Evaluation”, Proc., 9th Int’l Conf. on Fast Sea Transportation (FAST 2007), Shanghai, China.
- Gorski, W., Kulczyk, J. and Tabaczek, T., 2005, “The effect of limited depth and width of waterway on performance of ducted propellers”, Polish Maritime Research, Vol. 12, No. 4, pp. 3-9.
- Greco, L., Colombo, C., Salvatore, F. and Felli, M., 2006, “An Unsteady Inviscid Flow Model to Study Podded Propulsor Hydrodynamics”, Proc., TPOD – 2nd Int’l Conf. on Technological Advances in Podded Propulsion, L’aber Wrac’h, Brest, France.
- Greco, L. and Salvatore, F., 2006, “Numerical modelling of unsteady hydrodynamic characteristics of a propeller-rudder configuration”, Proc., 9th Int’l Symp. on Practical Design of Ships and Other Floating Structures (PRADS 2004), Luebeck- Travemunde, Germany.
- Hamill, G.A., Johnston, H.T., and Stewart, D.P., 1999, “Propeller wash scour near quay walls”, J. of Waterway, Port, Coastal and Ocean Engineering, pp. 170-175.
- Himei, K., Yamasaki, S., Yamasaki, M., Kudo, T. and Ukon, Y., 2006, “A proposal for a practical design method on supercavitating propellers”, Proc., 6th Int’l Symp. on Cavitation, Wageningen, The Netherlands.
- Hino, T. (ed.), 2005, The Proceedings of CFD WORKSHOP TOKYO 2005, National Maritime Research Institute, Tokyo, Japan.
- Hino, T., 2006, “CFD-based Estimation of Propulsive Performance in Ship Design”, Proc., 26th Symp. on Naval Hydrodynamics, Rome, Italy.
- Hoekstra, M., 2006, “A RANS-based Analysis Tool for Ducted Propeller Systems in Open Water Condition”, Int’l. Shipbuilding Progress, No. 53.
- Hsiao, C.T., Jain, A. and Chahine, G., 2006, “Effect of Gas Diffusion on Bubble Entrainment and Dynamics around a Propeller”, Proc., 26th Symp. on Naval Hydrodynamics, Rome, Italy.
- Hughes, A.W., Turnock, S.R. and Abu Sharkh, S.M., 2003, “Use of electromagnetic rim driven propulsor for waterjet propulsion systems”, RINA Trans. A: Int’l J. of Maritime Engineering, 145, (A4), 41-52.
- IMO, 2001, “IMO Adopts Convention on Control of Harmful Anti-fouling Systems on Ships”. Briefing 27/2001, Int’l Maritime Organization, London, <http://www.imo.org/>.
- Islam, M. F., Molloy, S.M., Veitch, B., Bose, N. and Liu, P., 2006, “Hydrodynamic Study of Podded Propulsors with Systematically Varied Geometry”, Proc., TPOD – 2nd Int’l Conf. on Technological Advances in Podded Propulsion, L’aber Wrac’h, Brest, France.
- ITTC 2002, “Testing and Extrapolation Methods Propulsion, Propulsor Open Water Test”, Proc., 23rd ITTC, Venice, Italy, ITTC Recommended Procedure 7.5-02-03-02.1, Revision 01.
- Jessup, S., Chesnakas, C., Fry, D., Donnelly, M., Black, S. and Park, J., 2004, “Propeller Performance at Extreme Off-Design Conditions”, Proc., 25th Symp. on Naval Hydro-

- dynamics, St John's, Canada.
- Jessup, S., Fry, D. and Donnelly, M., 2006, "Unsteady Propeller Performance in Crashback Conditions with and without a Duct", Proc., 26th Symp. on Naval Hydrodynamics, Rome, Italy.
- Kawamura, T., Ito, A. and Hinatsu, M., 2007, "Numerical Simulation of Bubbly Flow around a Marine Propeller", Proc., FEDSM2007, 5th Joint ASME/JSME Fluids Engineering Conf., San Diego, USA.
- Kawamura, T., Watanabe, T., Takekoshi, Y., Maeda, M., and Yamaguchi, H., 2004, "Numerical Simulation of Cavitating Flow around a Propeller" J. of Soc. of Naval Arch. of Japan, Vol. 195 (in Japanese).
- Kawanami, Y., Kudo, T. and Kawashima, H., 2005, "Contra-rotating podded propulsor and its full-scale model tests", Proc., 12th Int'l Congress of the Int'l Maritime Association of the Mediterranean (IMAM 2005), Lisboa, Portugal.
- Kerwin, J.E., 2006, "Hydrodynamic Issues in Waterjet Design and Analysis", Proc., 26th Symp. on Naval Hydrodynamics, Rome, Italy.
- Kerwin, J.E., Michael, T.J. and Neely, S.K., 2006, "Improved Algorithms for the Design/Analysis of Multi-Component Complex Propulsors", Proc., Propeller/ Shafting 2006 Symposium, SNAME.
- Kim, J. and Chung W.K., 2006, "Accurate and practical thruster modelling for underwater vehicles", Ocean Engineering, Vol. 33, pp. 566-586.
- Kim, J., Kim, K.S., Kim, G.D., Park, I.R., Van, S.H., 2006, "Hybrid RANS and potential based numerical simulation for self-propulsion performances of the practical container ship", J. of Ship & Ocean Technology, Vol. 10, No. 4.
- Kim, J., Park, I.R. and Van, S.H., 2005, "RANS Computations for KRISO Container Ship and VLCC Tanker using the WAVIS code", Proc., CFD Workshop Tokyo 2005, Tokyo, Japan.
- Kim, K.S., Kim, J., Park, I.R., Kim, G.D. and Van, S.H., 2007, "RANS Analysis for Hull-Propeller-Rudder Interaction of a Commercial Ship by Using the Overset Grid Scheme", Proc., 9th Int'l Conf. on Numerical Ship Hydrodynamics, Ann Arbor, USA.
- Kinnas, S.A., 2006, "Prediction of Performance and Design of Propulsors – Recent Advances and Applications", Proc., TPOD – 2nd Int'l Conf. on Technological Advances in Podded Propulsion, L'aber Wrac'h, Brest, France.
- Kinnas, S., Lee, H., Michael, T. and Sun, H., 2007, "Prediction of Cavitating Waterjet Propulsor Performance Using a Boundary Element Method", Proc., 9th Int'l Conf. on Numerical Ship Hydrodynamics, Ann Arbor, USA.
- Korkut, E., 2007, "An Investigation into the Effects of Foul Release Coating on Propeller Performance, Noise and Cavitation Characteristics", Report of School of Marine Science and Technology in Newcastle University, Report No: MT-2007-004.
- Kosuhan, K., 2006, "Dynamics of ventilated propeller blade loading on thrusters due to forced sinusoidal heave motion", Proc., 26th Symp. on Naval Hydrodynamics, Rome, Italy.
- Krasilnikov, V., Berg, A., Yin, S.J., Achkinadze, A.S. and Ponkratov, D.V., 2006, "Possibilities of a Viscous/Potential Coupled Method to Study Scale Effects on Open-Water Characteristics of Podded Propulsors", TPOD – 2nd Int'l Conf. on Technological Advances in Podded Propulsion, L'aber Wrac'h, Brest, France.



- Krasilnikov, V.I., Zhang, Z., Hong, F., Ponkratov, D.V. and Sun, J.Y., 2007, "Steady Analysis of Viscous Flow around Ducted Propellers: Validation and Study on Scale Effects", Proc., 9th Int'l Conf. on Fast Sea Transportation FAST2007, Shanghai, China.
- Kuiper, G., 1994, "Effect of skew and rake on cavitation inception for propeller blades with thick blade sections", Proc., 20th Symp. on Naval Hydrodynamics, Santa Barbara, U.S.A.
- Kuiper, G., van Terwisga, T.J.C., Zondervan, G.J., Jessup, S.D. and Krikke, E.M., 2006, "Cavitation inception tests on a systematic series of two blade propellers", Proc., 26th Symp. on Naval Hydrodynamics, Rome, Italy.
- Lababidy, S.L., Di Felice, F.D., Bose, N., and Liu, P., 2006, "Evaluation of a Dynamic Positioning Thruster Performance Characteristics With and Without a Nozzle", Proc., 26th Symp. on Naval Hydrodynamics, Rome, Italy.
- Lan, C.E., 1974, "A Quasi-Vortex-Lattice Method in Thin Wing Theory", J. of Aircraft, Vol. 11, No. 9.
- Lavis, D.R., Forstell, B.G., and Purnell, J.G., 2007, "Compact Waterjets for High-Speed Ships", Ships and Offshore Structures, Vol. 2, Issue 2, pp. 115 – 125 (also in Proc. 5th Int'l Conf. on High Performance Marine Vehicle, 8-10 Nov. 2006, Australia).
- Lee, H.S. and Kinnas, S.A., 2006, "Prediction of Cavitating Performance of Ducted Propeller", Proc. 6th Int'l Symp. on Cavitation CAV2006, Wageningen, The Netherlands.
- Li, D.Q., Berchiche, N. and Janson, C.E., 2006, "Influence of Turbulence Models on the Prediction of Full-Scale Propeller Open Water Characteristics with RANS methods", Proc., 26th Symp. on Naval Hydrodynamics, Rome, Italy.
- Ligtelijn, J.T., van Wijngaarden, H.C.J., Moulijn, J.C. and Verkuyl, J.B., 2004, "Correlation of Cavitation: Comparison of Full-Scale Data with Results of Model Tests and Computations", Proc. SNAME Annual Meeting, Washington D.C., USA.
- Lübke, L.O., 2005, "Numerical Simulation of the Flow around the Propelled KCS", Proc. CFD Workshop Tokyo 2005, Tokyo, Japan.
- Lübke, L.O. and Mach, K.P., 2004, "LDV measurements in the wake of the propelled KCS model and its use to validate CFD calculation", Proc. 25th Symp. on Naval Hydrodynamics, St. John's, Canada.
- Michael, T. J. and Chesnakas, C. J., 2004, "Advanced Design, Analysis, and Testing of Waterjet Pumps", Proc., 25th Symp. on Naval Hydrodynamics, St. John's Canada.
- Minami, Y. and Kawanami, Y., 2005, "On the Research and Development of Super ECO-Ship Project", Proc., Int'l Offshore and Polar Engineering Conference (ISOPE 2005), Seoul, Korea.
- Mittal, R., Bozkurtas, M., Dong, H., Lauder, G. and Madden, P., 2006, "Hydrodynamic Performance of Deformable Fish Fins with Application to Bio-Robotic Autonomous Underwater Vehicles", Proc., 26th Symp. on Naval Hydrodynamics, Rome, Italy.
- Molland, A.F., and Turnock, S.R., 2007, Marine rudders and control surfaces: principles, data, design and applications, Butterworth-Heinemann, p.219-222.
- Mouritz, A., Gellert, E., Burchil, P. and Challis, K., 2001, "Review of advanced composite structures for naval ships and submarines", Composite Structures, Vol. 53, pp. 21-41.
- Muller, S.B. and Abdel-Maksoud, M., 2007, "Numerical Investigation of Transverse Thrusters", Proc., STG-Sprechttag –CFD in Ship Design, TUHH, Hamburg.

- Mutton, R.J., Atlar, M., Downie, M. and Anderson, C.D., 2005, "Drag Prevention Coatings for Marine Propellers", Proc., 2nd Int'l Symp. on Seawater Drag Reduction, Busan, Korea.
- Nakatake, K., 1981, "A Practical Method to Calculate Propulsive Performance of Ships", Memoirs of Faculty of Engineering, Kyushu U., Vol. 41, No. 1.
- Neely, S.K., 1997, "Non-Cylindrical Blade Geometry", Proc., Propellers/ Shafting '97 Symp., SNAME.
- Neely, S.K. 1998, "Application of NURBS Surfaces for Propeller Geometry", Proc., 25th American Towing Tank Conference, Iowa City, Iowa.
- Newton, R. and Rader, H., 1961, "Performance data of propellers for high-speed craft", Trans. RINA 103 (2), pp. 93-129.
- Nielsen, B., 2005, "Bow thruster-induced damage: a physical model study on bow thruster induced flow", MSc Thesis, Hydraulic Engineering, Delft University.
- Nozawa, K. and Takayama, N, 2005, "A research on propulsive performance of high speed craft equipped with surface piercing propellers", Proc., Int'l Conf. on Fast Sea Transportation, St. Petersburg, Russia.
- Okada, Y., Yoshioka, M., Fujita, T. and Watanabe, K., 2000, "Experimental Study on Surface Piercing Propeller", J. of Soc. of Naval Arch. of Japan, Vol. 188 (in Japanese).
- Oweis, G.F., Fry, D., Chesenakas, C.J., Jessup, S.D. and Ceccio, S.L., 2006a, "Development of a tip-leakage flow- Part 1: The flow over a range of Reynolds numbers", J. of Fluids Engineering, Vol. 128.
- Oweis, G.F., Fry, D., Chesenakas, C.J., Jessup, S.D. and Ceccio, S.L., 2006b, "Development of a tip-leakage flow- Part 2: Comparison between the ducted and unducted rotor", J. of Fluids Engineering, Vol. 128.
- Paik, B.G., Kim, J., Park, Y.H., Kim, K.S., Yu, K.K., 2007, "Analysis of wake behind a rotating propeller using PIV technique in a cavitation tunnel", Ocean Engineering, Vol. 34, pp. 594-604.
- Paik, B.G., Kim, K.Y., Ahn, J.W., Kim, Y.S., Kim, S.P., and Park, J.J., 2008, "Experimental study on the gap entrance profile affecting rudder gap cavitation", Ocean Engineering, Vol. 35, pp. 139-149.
- Palmer, A., Hearn, G.E. and Stevenson, P., 2008, "Modelling tunnel thrusters for autonomous underwater vehicles", Proc., IFAC workshop on navigation, guidance and control of underwater vehicles, Killaloe, Ireland.
- Park, W.G., Jung, Y.R., and Kim, C.K., 2005, "Numerical flow analysis of single-stage ducted marine propulsor", Ocean Engineering, Vol. 32, pp.1260-1277.
- Rogers, D.F. and Adams, J.A., 1990, Mathematical Elements for Computer Graphics, 2nd edition, McGraw Hill, New York.
- Ruth, E. and Smogeli, O.N., 2006, "Ventilation of Controllable Pitch Thrusters", Marine Technology, Vol. 43, No. 4, pp. 170-179.
- Sampaio, C.M.P., Russo, A. A., Nishimoto, K., and Hirata, K., 2005, "Full-scale resistance study and analysis of a patrol boat at three different hull/propeller roughness conditions", Proc., 12th Int'l Congress of the Int'l Maritime Assoc. of the Mediterranean (IMAM 2005), Lisboa, Portugal.
- Sánchez-Caja A., Sipilä T. and Pylkkänen J., 2006a, "Simulation of the Incompressible Viscous Flow around an Endplate Propeller Using a RANSE Solver", Proc., 26th Symp. on Naval Hydrodynamics, Rome, Italy.



- Sánchez-Caja, A., Veikonheimo, T. and Pylkanen, J.V., 2006b, "RANS Predictions for Flow Patterns Around a Compact Azipod", TPOD – 2nd Int'l Conf. on Technological Advances in Podded Propulsion, L'aber Wrac'h, Brest, France.
- Sasaki, N., Kawanami, Y., Ukon, Y., Kano, T. and Tomizawa, S., 2006, "Model Test Procedure and Analysis of Hybrid CRP POD System", TPOD – 2nd Int'l Conf. on Technological Advances in Podded Propulsion, L'aber Wrac'h, Brest, France.
- Sfakiotakis, M., Lane, D. M., Bruce, J. and Davies, C., 1999, "Review of Fish Swimming Modes for Aquatic Locomotion", IEEE Journal of Oceanic Engineering, Vol. 24, No. 2.
- Shen, Y., 1996, Dual cavitating hydrofoil structures, Tech. rep., US Patent Number 5,551,369.
- Simonsen, C.D. and Stern, F., 2005, "RANS Maneuvering Simulation of Esso Osaka With Rudder and a Body-Force Propeller", J. of Ship Research, Vol. 49, No. 2.
- Stauble, U., 2007, "Advances in Submarine Propulsion", Naval Forces, Vol. 28, ISSN 0722-8880 Special Issue.
- Tahara, Y., Wilson, R. and Carrica, P., 2005, "Comparison of Free-Surface Capturing and Tracking Approaches in Application to Modern Container Ship and Prognosis for Extension to Self-Propulsion Simulator", Proc. of CFD WORKSHOP TOKYO 2005, Tokyo, Japan.
- Takada, N., Hoshino, T., Ishikawa, S. and Higaki, S., 2002, "Simulation of free-surface viscous flow around practical hull and rudder with propeller effects", J. Soc. of Naval Arch. of Japan, Vol. 192 (in Japanese).
- Thomas, T., and Schmode, D., 2005, "Computation of bow thrusters with RANS-Solver FreSCo", Proc., 8th Numerical Towing Tank Symposium, 3pp.
- Turnock, S.R., Pashias, C. and Rogers, E., 2006, "Flow feature identification for capture of propeller tip vortex", Proc., 26th Symp. on Naval Hydrodynamics, Rome, Italy
- Tzabiras, G.D., 2004, "Resistance and self-propulsion simulations for a Series-60, Cb=0.6 hull at model and full scale", Ship Technology Research, Vol. 51.
- Ukon, Y., Sasaki, N., Fujisawa, J. and Nishimura, E., 2006, "The Propulsive Performance of Podded Propulsion Ships with Different Stern Shape", Proc., TPOD – 2nd Int'l Conf. on Technological Advances in Podded Propulsion, L'aber Wrac'h, Brest, France.
- Van S.H. and Yoon, H.S., 2002, "Investigation on the Powering Performance Prediction for Azimuth Thrusters", Journal of Ship & Ocean Technology, Vol. 6, No.1.
- Veikonheimo T., 2006, "Solving Problems of Propeller Model Scaling", The Naval Architect, (July/August).
- Vysohlid, M. and Mahesh, K., 2006, "Large Eddy Simulation of Crashback in Marine Propellers", Proc., 26th Symp. on Naval Hydrodynamics, Rome, Italy.
- Wood and Harris, 1920, "Some notes on the theory of an airscrew working in a wind channel", Aeronautical Research Council R&M 662.
- Yamasaki, S. and Okazaki, A., 2005, "Cavitation test on a straight leading edge propeller and a tip rake propeller", J. of Japan Soc. of Naval Arch. and Ocean Eng., Vol. 2 (in Japanese).
- Yamasaki, S. and Okazaki, A., 2007, "Design and model tests of a backward tip rake propeller for a low speed ship" J. of Japan Soc.

of Naval Arch. and Ocean Eng., Vol. 5 (in Japanese).

Yamazaki, R., 1968, "On the Propulsion Theory of Ships on Still Water –Introduction–", Memoirs of Faculty of Engineering, Kyushu U., Vol. 27, No. 4.

Young Y.L., 2004, "Hydroelastic Modeling of Surface-Piercing Propellers", Proc., 25th Symp. on Naval Hydrodynamics, St John's, Canada.

Young Y.L., 2006, "Hydroelastic response of composite marine propellers", Proc., Propeller/Shafting 2006 Symposium, SNAME.

Young, Y.L., 2007, "Time-dependent hydroelastic analysis of cavitating propulsors," J. of Fluids and Structures, Vol. 23, pp 269–295.

Young Y.L., Michael T.J., Seaver M. and Trickey S.T., 2006, "Numerical and Experimental Investigations of Composite Marine Propellers", Proc., 26th Symp. on Naval Hydrodynamics, Rome, Italy.

Young, Y.L. and Shen, Y.T., 2007, "A Numerical Tool for the Design/Analysis of Dual-Cavitating Propellers", J. of Fluids Engineering, Vol. 129, No. 6, pp. 720-730.

Zhang, X.Q., Wang, Z.D. and Zhang, Z.S., 2006, "Hydrodynamic study of bionic propulsion for 2-D flapping foil", J. of Hydrodynamics, Ser. A (in Chinese), Vol. 21, No. 5.

Zondervan G.V., Hoekstra, M. and Holtrop J., 2006, "Flow Analysis, Design and Testing of Ducted Propellers", Proc., Propellers/Shafting 2006 Symposium, Virginia, USA.